Geophysics Interferometer (GIF) subgroup

Akiteru Takamori (sub-chief)
(ERI, University of Tokyo)

- Construction and operation of GIF for geophysical observations
- Data analysis and interpretation (including environmental sensors)
- Application of GIF data for improving KAGRA's performance


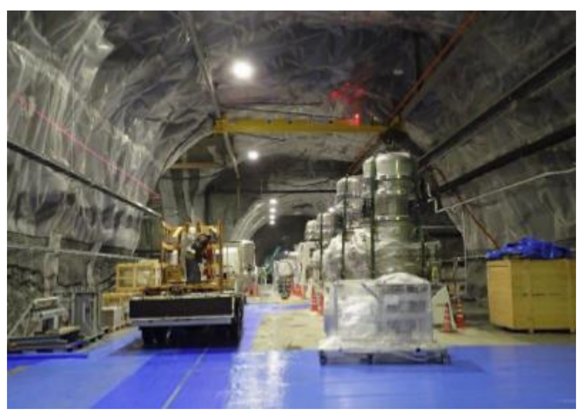

Strainmeter observes slow ground motion

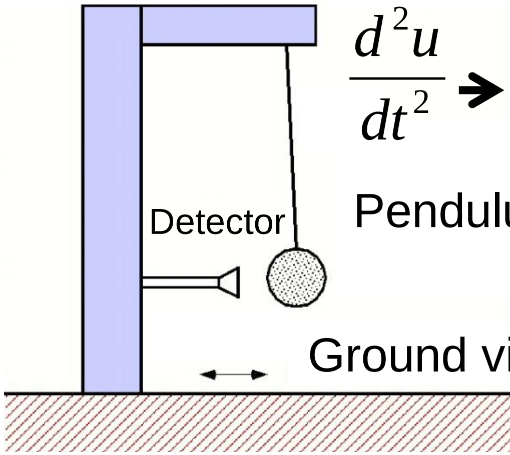

$$\frac{d^2u}{dt^2} \rightarrow \frac{du}{dt}$$

Pendulum

Seismometer:

Inertial sensor with cut-off f_c

$$\frac{u(x+dx)-u(x)}{L} \cong \frac{\partial u}{\partial x}$$

Strainmeter:

Measures distance between separated points

Reference rod made of quartz or invar

Detection of low-frequency waves

conventional strainmeter

Laser strainmeter

- Laser wavelength: absolute length reference

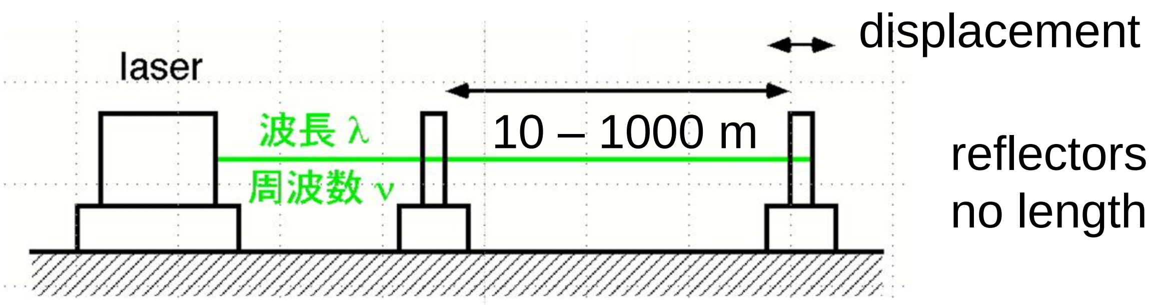

reflectors fixed to ground
no length / alignment controls

- Michelson interferometer

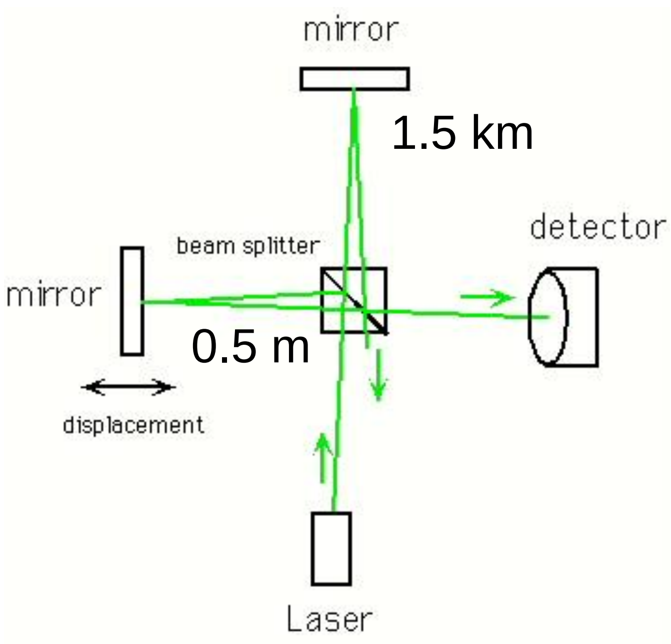

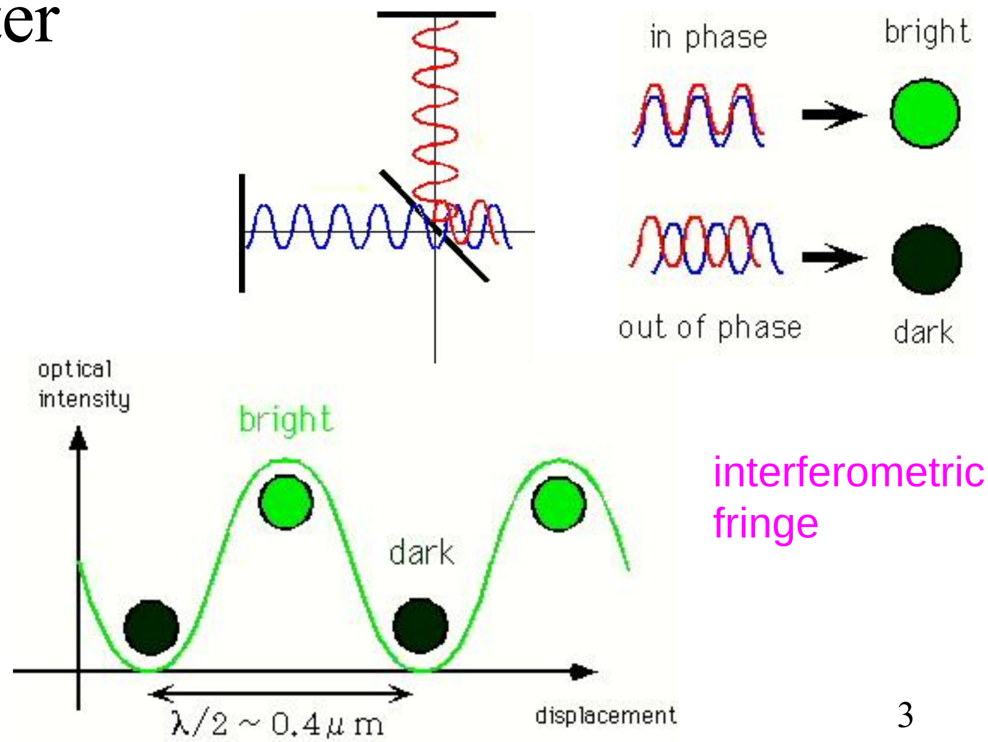

interferometric fringe

Construction of GIF

Construction of a 1500-m laser strainmeter in the KAGRA tunnel

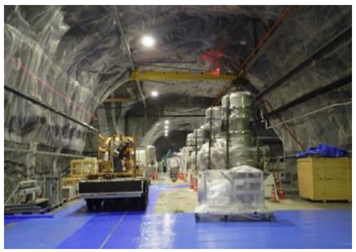

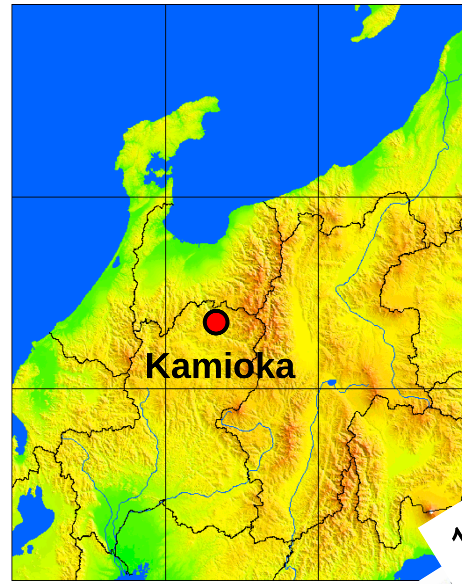

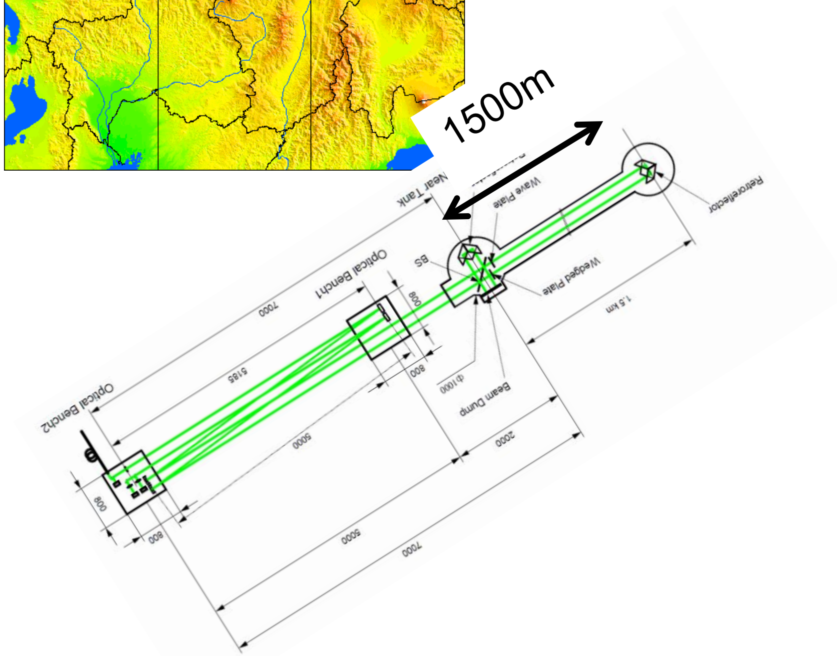

GIF & clio strainmeters

- GIF in KAGRA tunnel (in operation since 2016)
- 100 m strainmeter in CLIO site (since 2003)

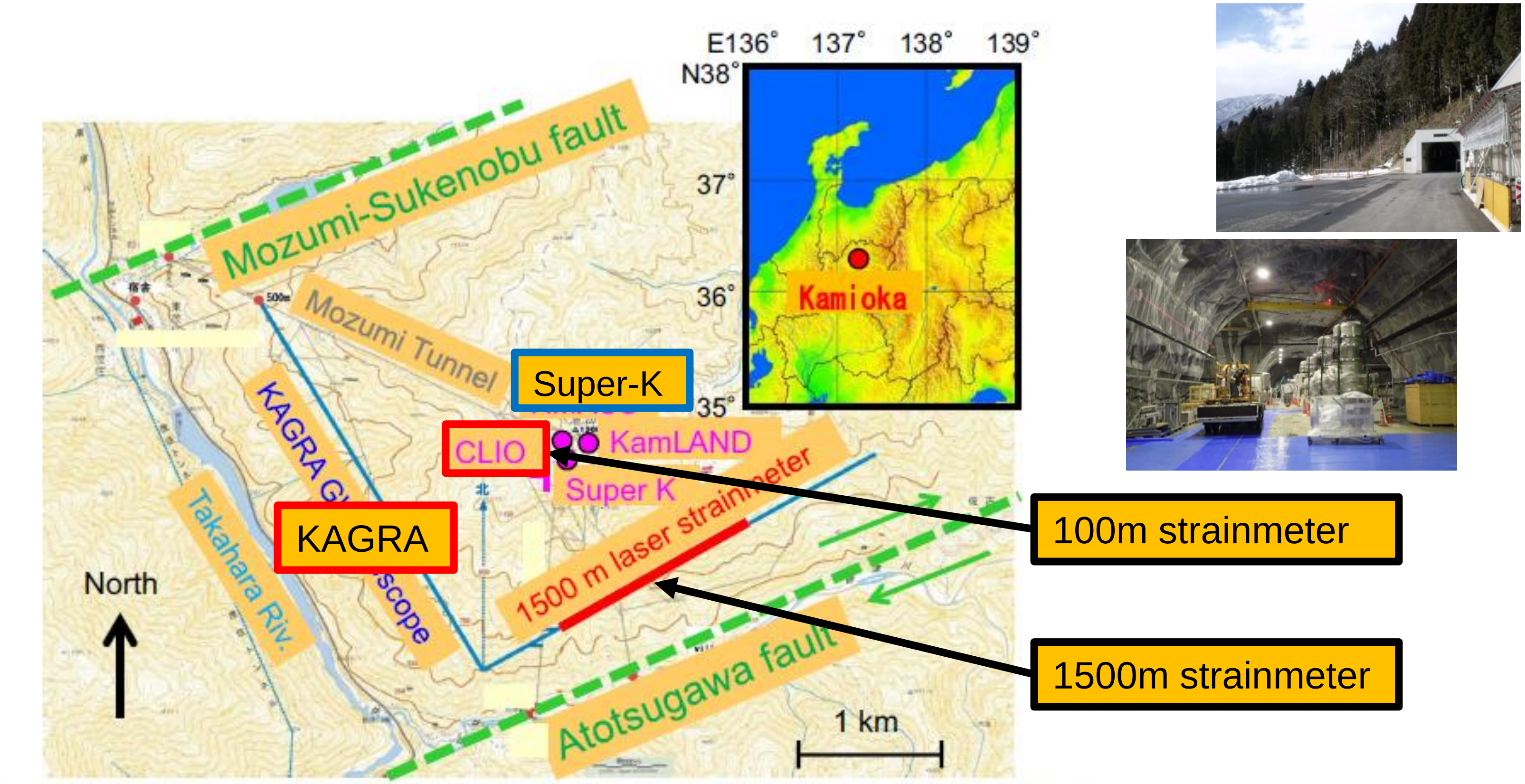

KAGRA baselines and fault locations
(Cosmic Ray Research Institute, Univ. of Tokyo)

Optical configuration of GIF–X

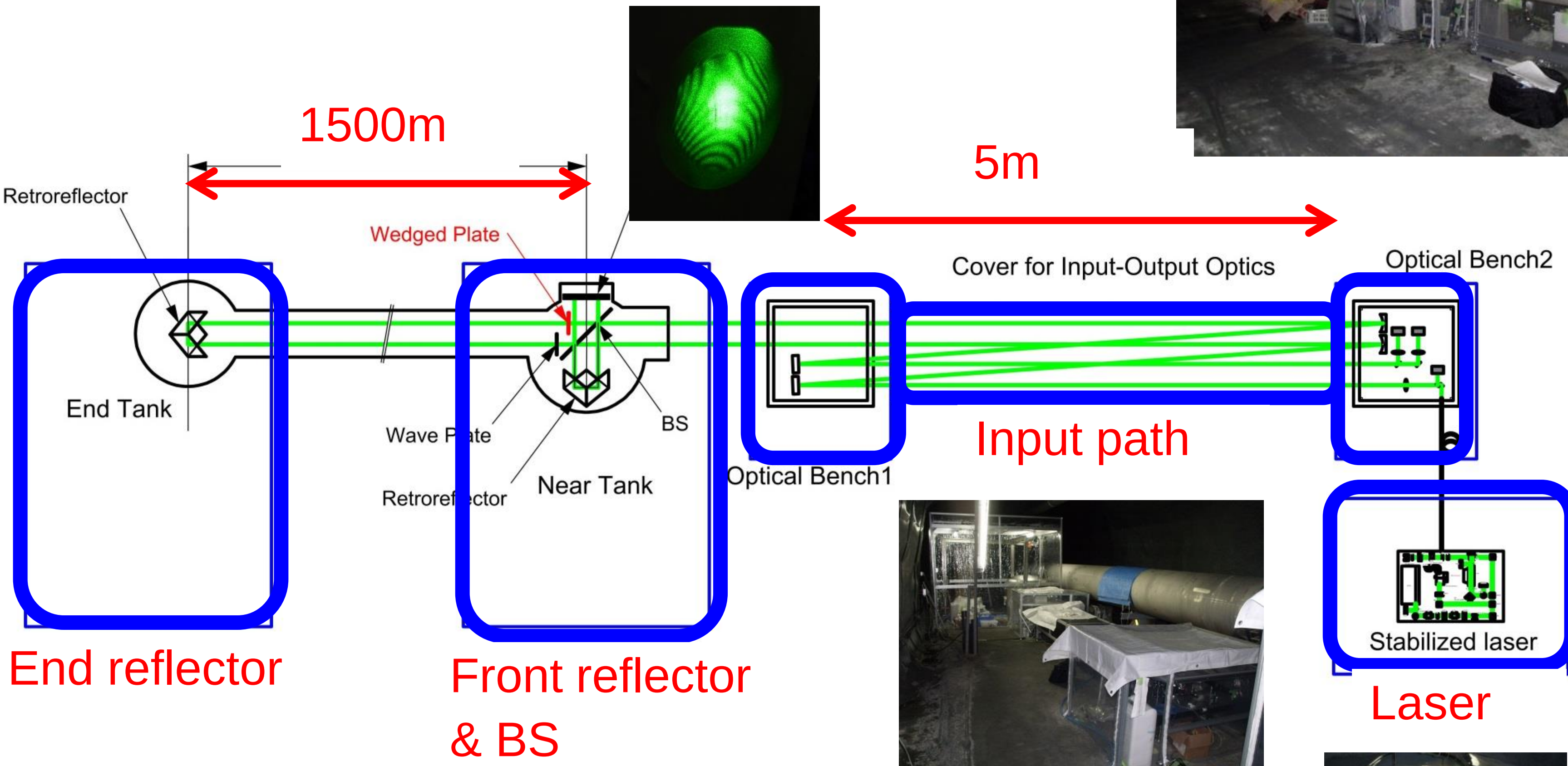

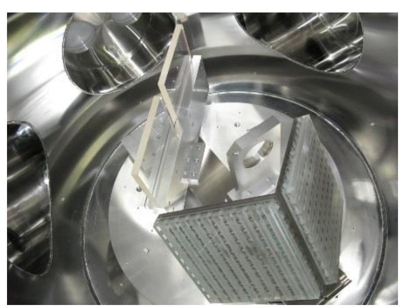

Iodine (I_2) stabilized laser

- Stabilizes laser frequency
  - To iodine Doppler-free hyperfine absorption line (532 nm)
  - Stability of ~ 10^{-13} absolute frequency in Allan variance estimation

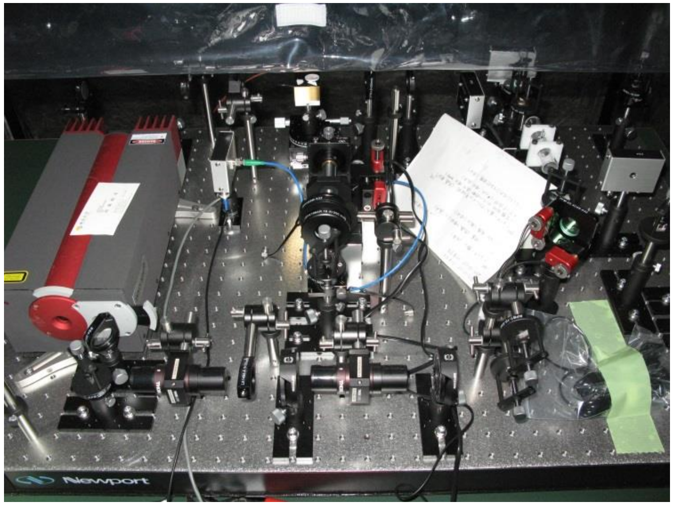

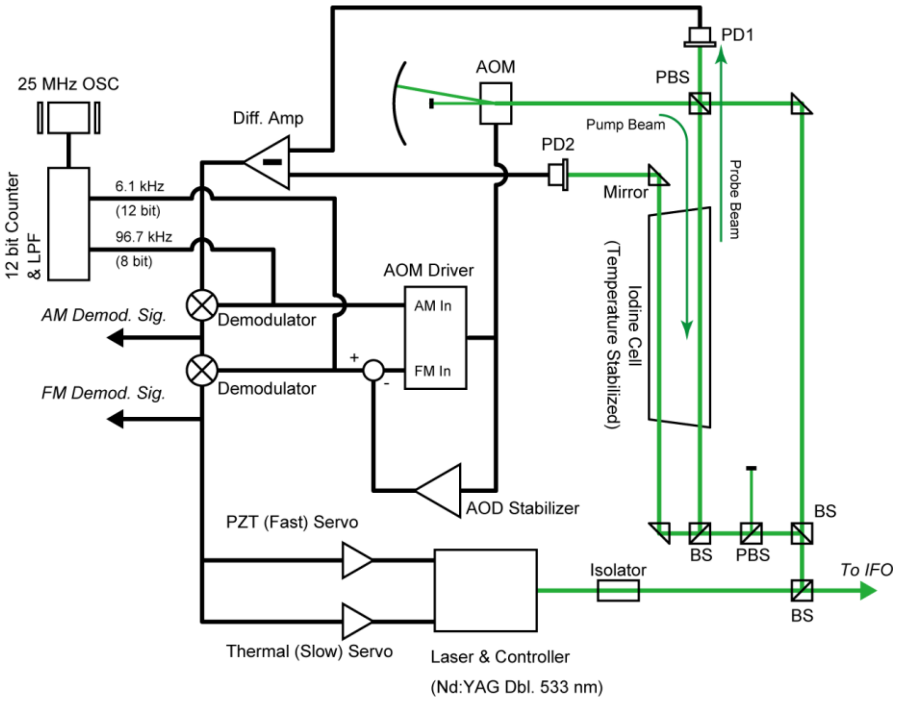

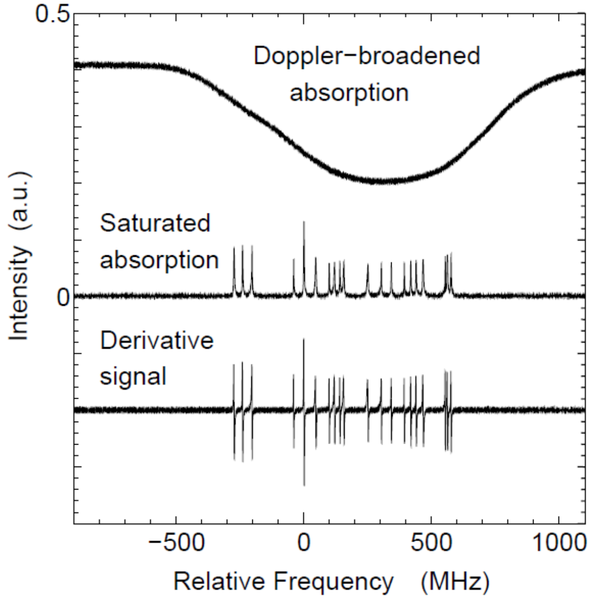

Input & output optical system

- Input & output telescopes
  - Optimizes input beam profile
  - Focuses output beam to PDs for fringe detection

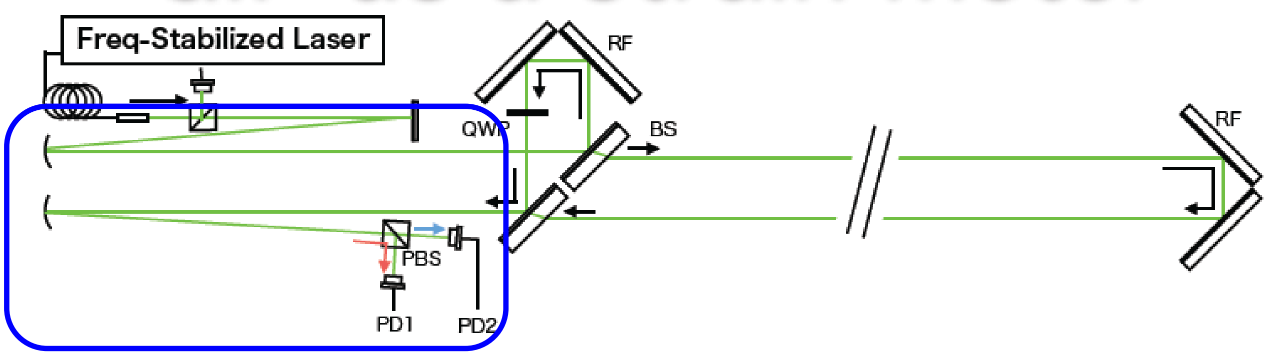

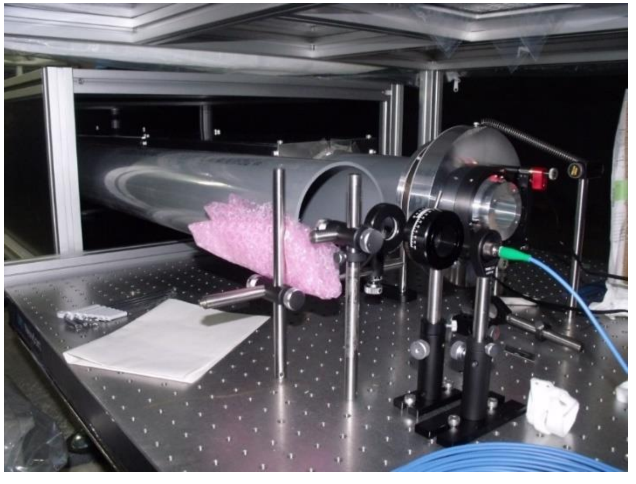

Input optics (left) and interferometric fringe (right).

Retroreflectors (corner reflectors)

- Installed at both arm ends
  - 3 mutually perpendicular mirrors
  - Reflect beam exactly parallel to incident beam
  - reflectors with 15-inch aperture were specially manufactured for GIF

    cf. clio (100 m strainmeter) uses 6-cm reflectors (standard size)

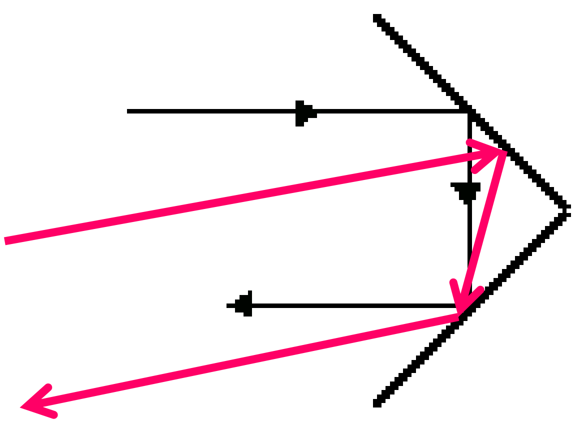

Retroreflector for clio

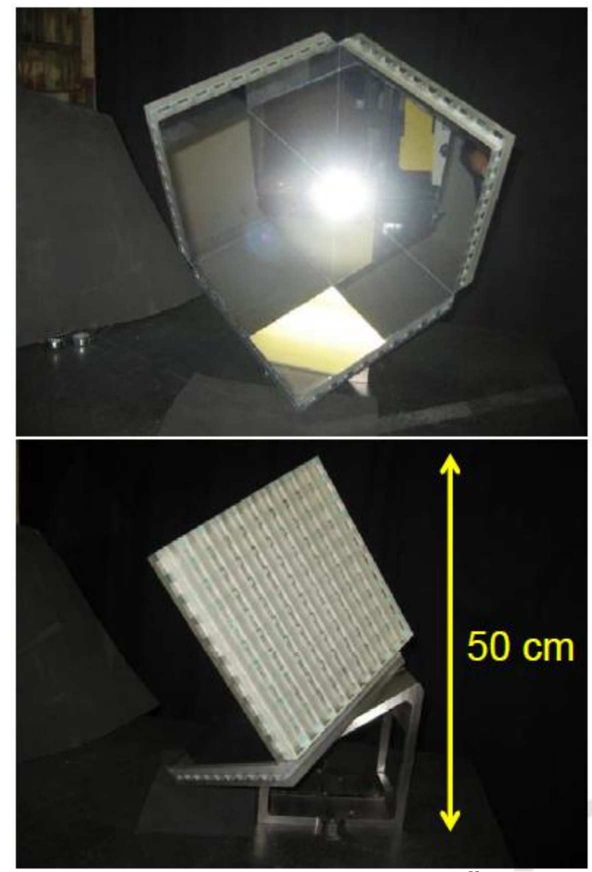

Retroreflector for GIF

Observation with GIF

- **Earth tides – $\sim 3 \times 10^{-8}$ in strain**
  - Observed amplitude – 87 % of theoretical calc.
  - Earth tides are reduced by topographic effect

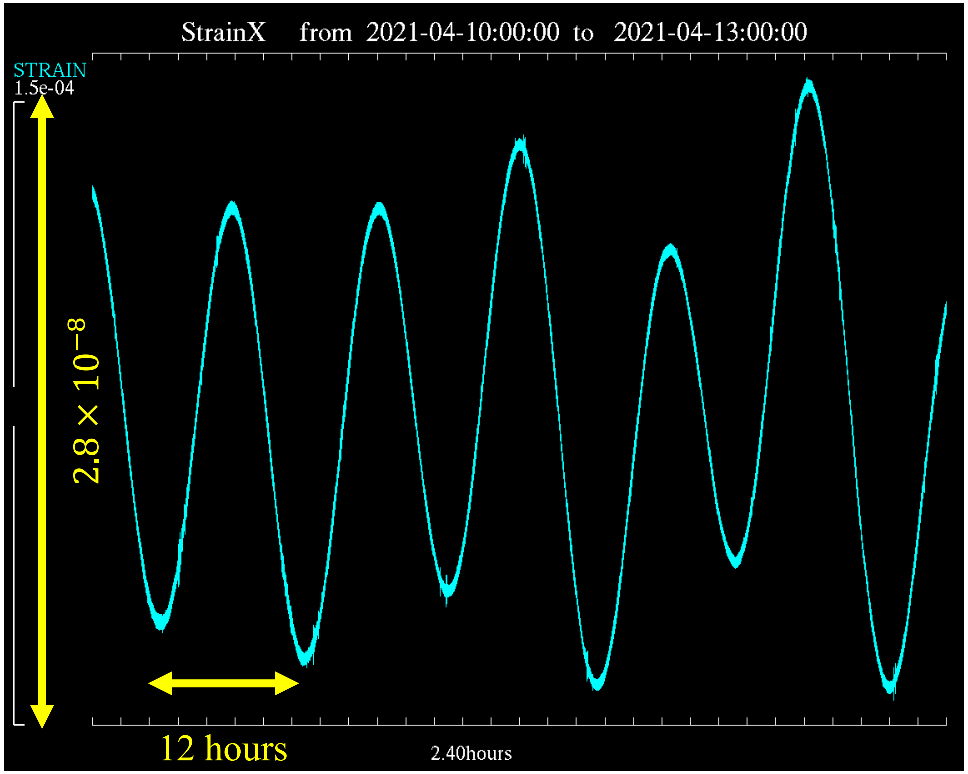

Earth tide

- **Deformation of the Earth caused by gravity of the Moon and Sun**

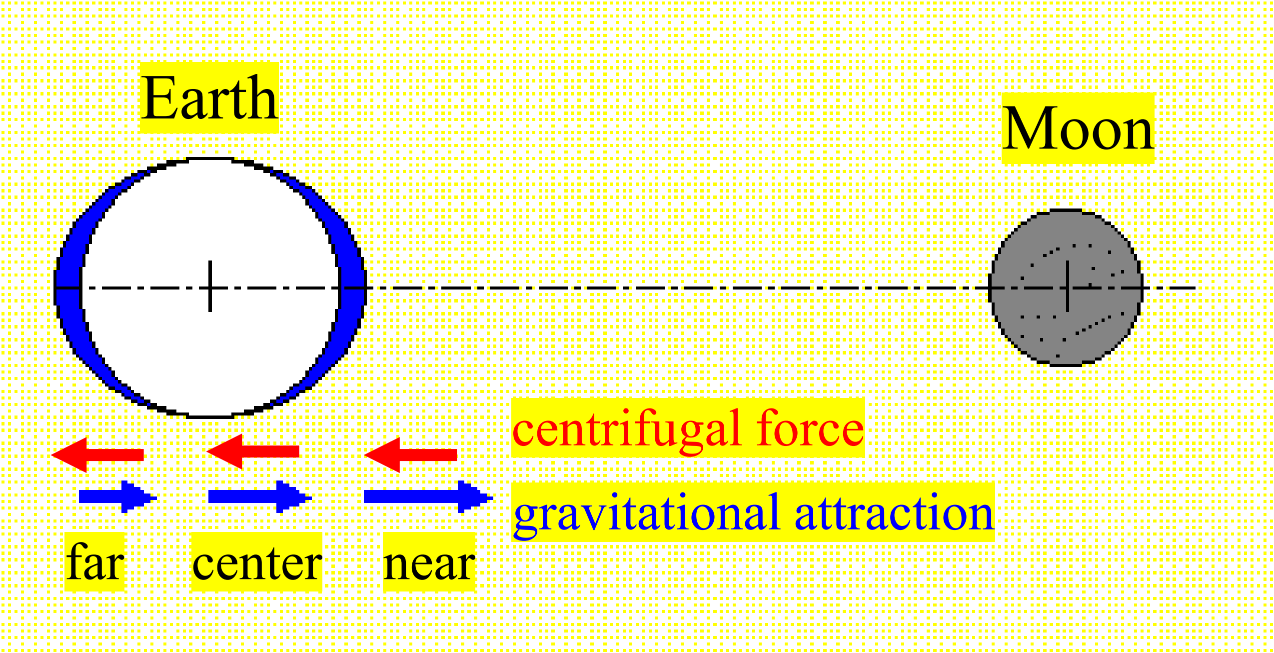

Nominal displacement: 3 μm / 100 m (3×10^{-8} in strain)

Diameter of hair – 50 μm (typical)

Ground motion is our SIGNAL.

- Earth tides
  - Earth's rigidity, inner structure, oceanic & topographic effects…

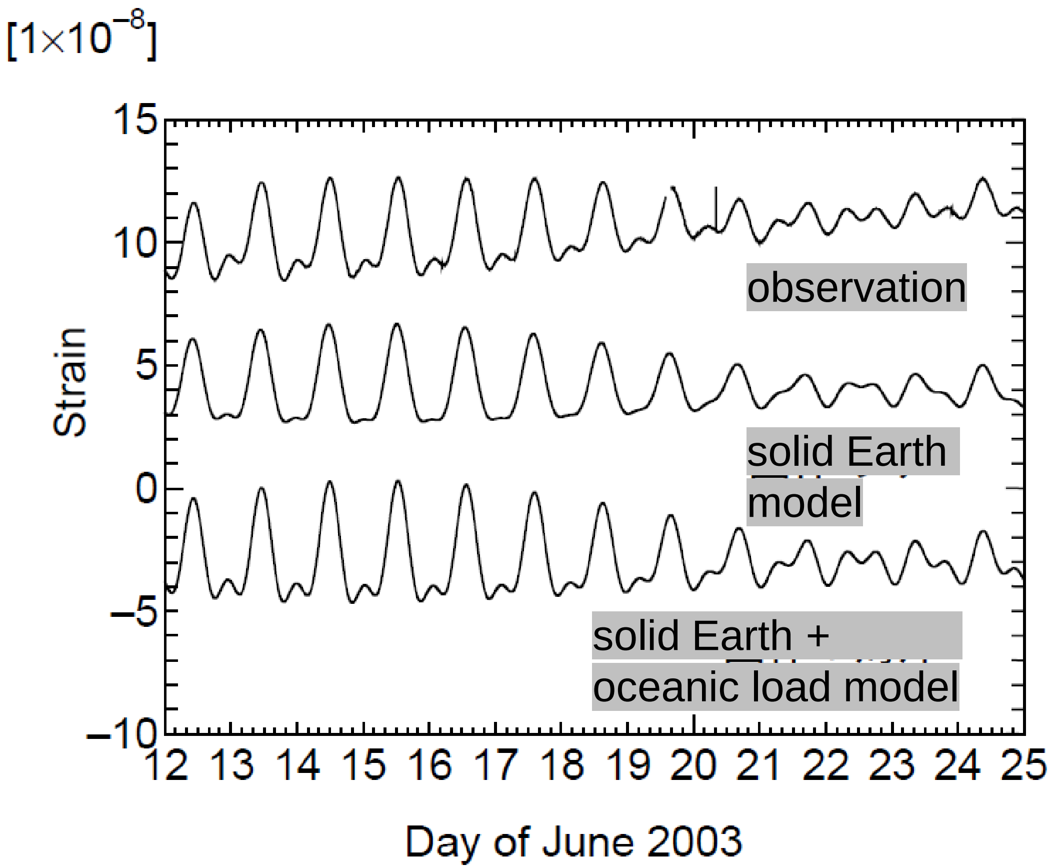

Good agreement between observation and standard solid Earth model + oceanic load + topographic effect (mountain)

→ Research on inner structure of Earth

Observed Earth tides (left) and topographic effects of underground site

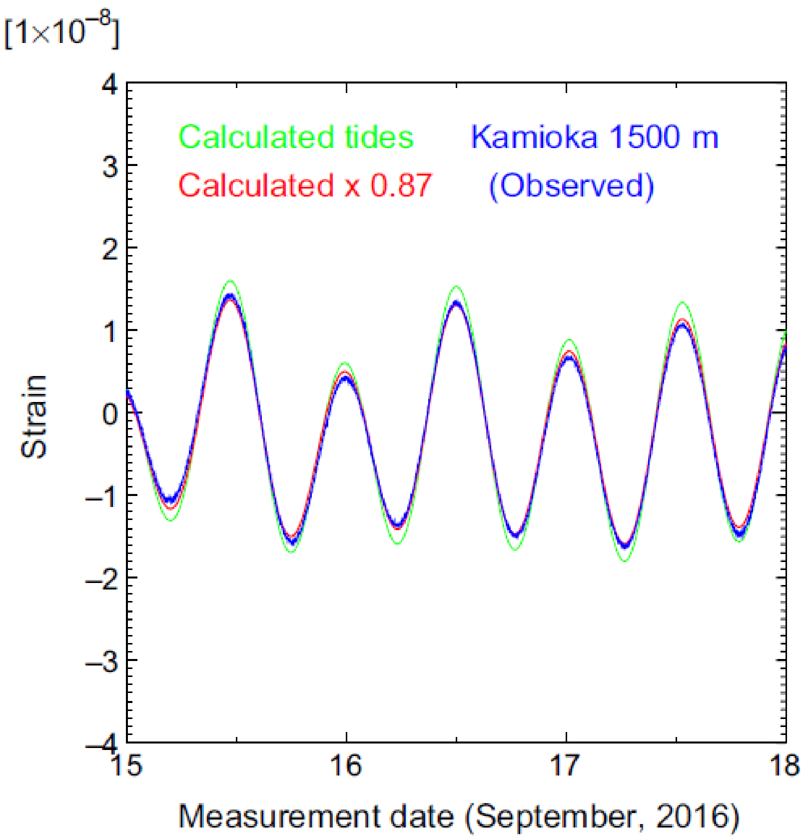

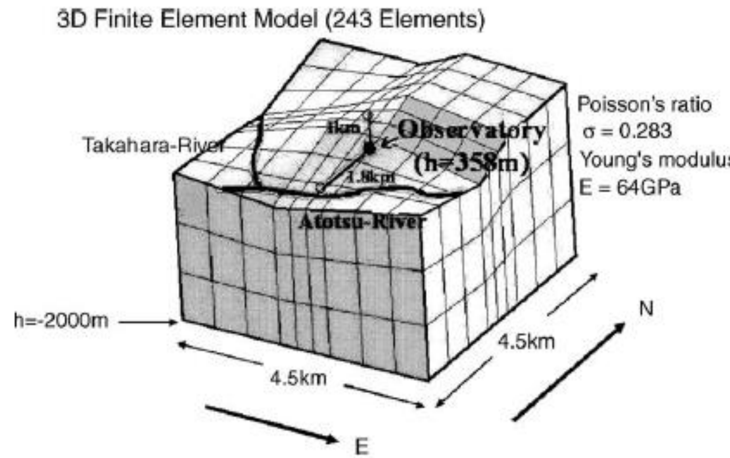

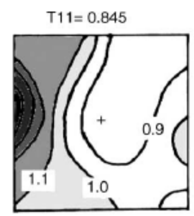

$$\varepsilon_{\mathrm{NS}} = 0.901 e_{\mathrm{NS}} + 0.006 e_{\mathrm{EW}} + 0.009 e_{\mathrm{NS-EW}}$$

$$\varepsilon_{\mathrm{EW}} = -0.011 e_{\mathrm{NS}} + 0.845 e_{\mathrm{EW}} + 0.025 e_{\mathrm{NS-EW}}$$

Reduction of tidal amplitude due to topography, 80-90% (Takemoto, 2006)

Large and distant earthquakes

- Fiji earthquake (2018)
  - maximum strain amplitude at Kamioka $\sim 3.9 \times 10^{-8}$

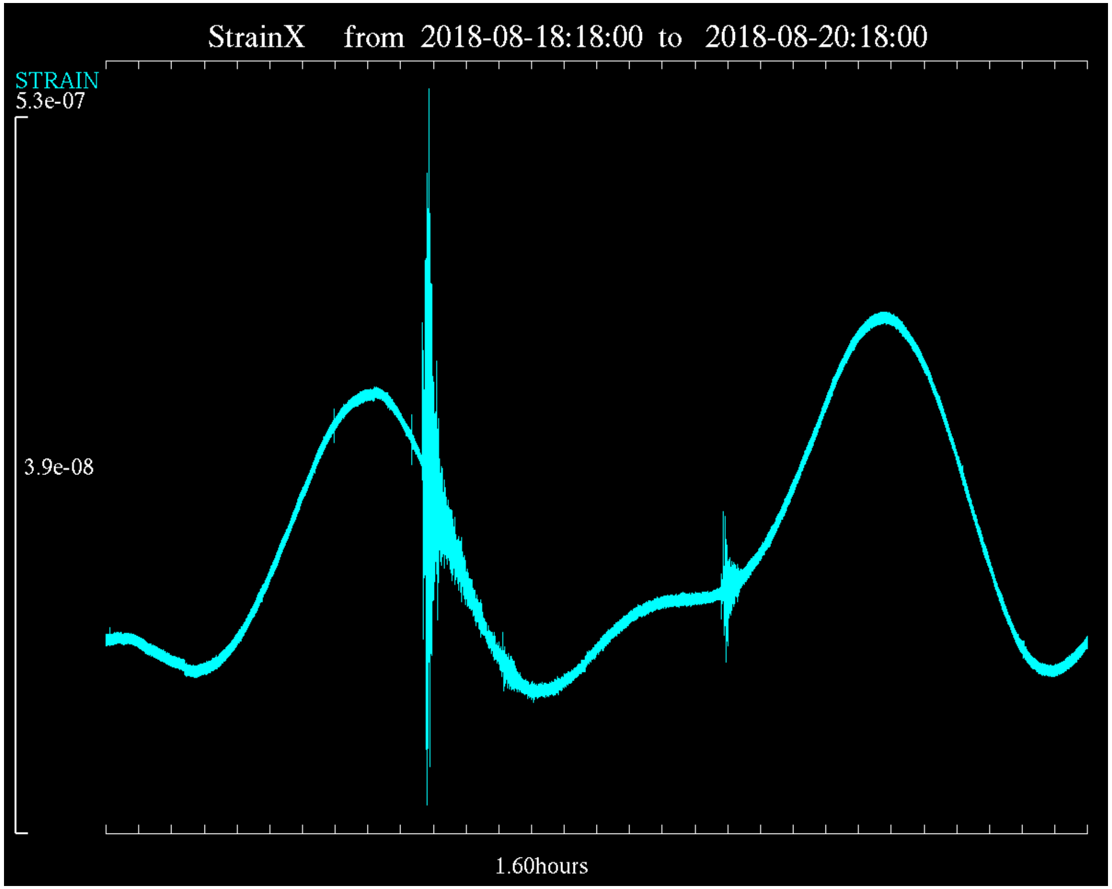

Earthquake waveforms observed by GIF

19-AUG-2018 00:19:37 M8.2 Fiji Islands

19-AUG-2018 14:56:28 M6.9 Sumbawa, Indonesia

Near earthquakes

- Fukushima (22-NOV-2016 6:59:49, M6.9)
  - maximum strain amplitude at Kamioka $\sim 3 \times 10^{-7}$

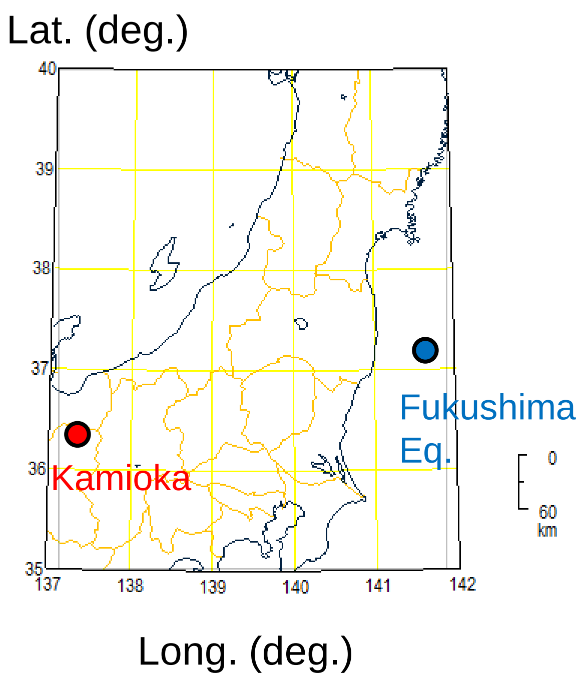

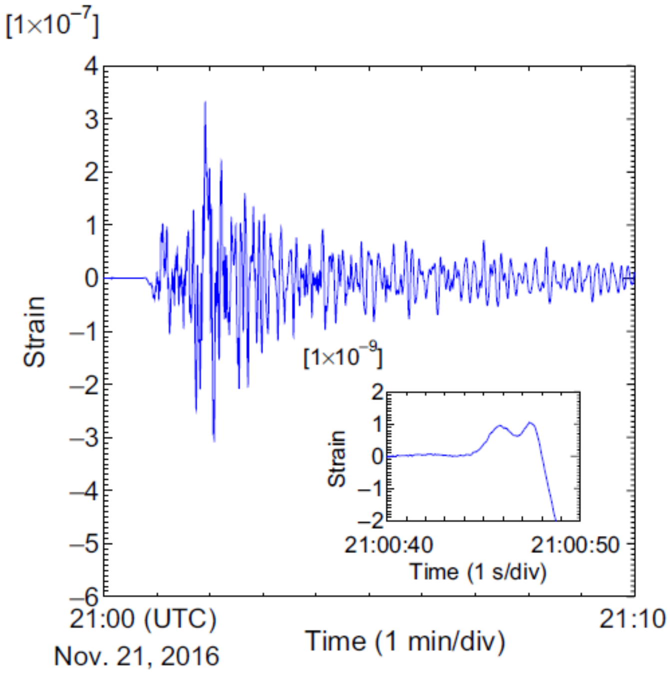

Coseismic strain changes

- Crustal deformations associated with seismic fault rupture
  - 10^{-9} → 1.5 km baseline shrinks 1.5 μm…Study on mechanism of earthquakes

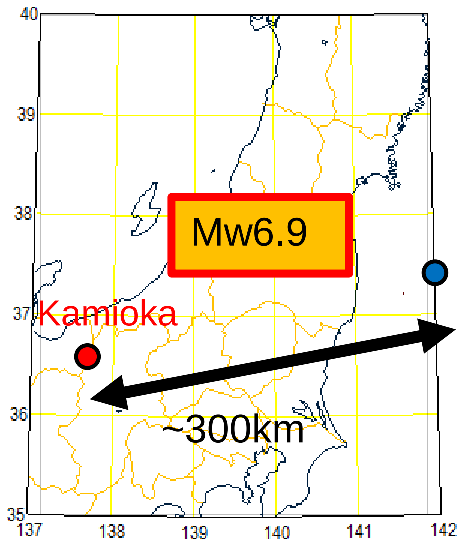

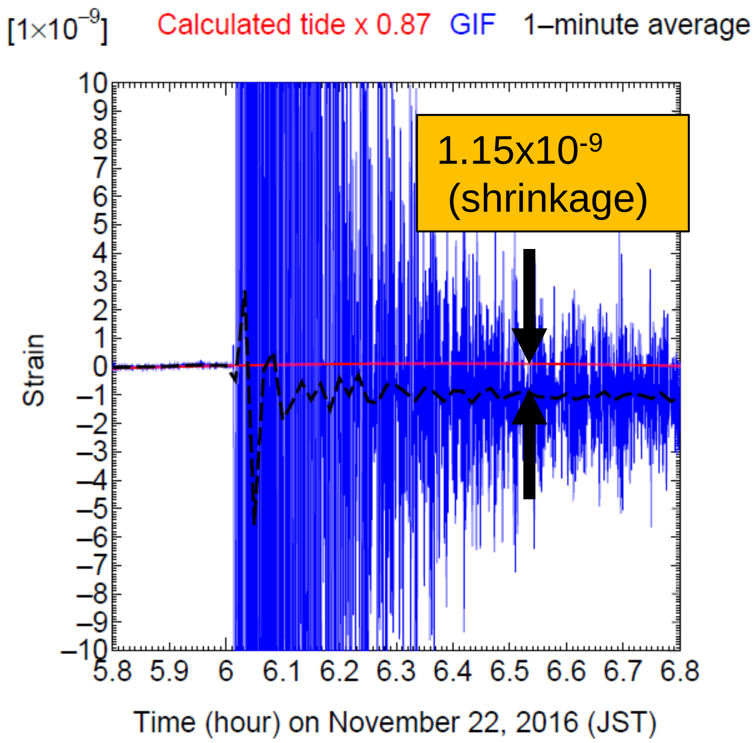

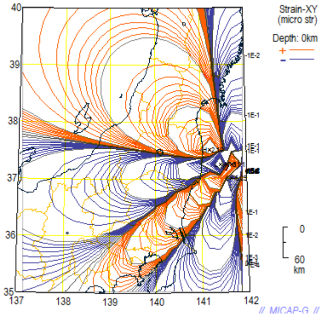

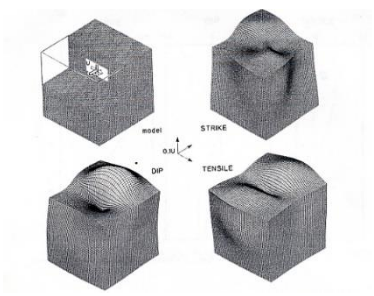

Strain spectra

- Lowest background, especially at around (1 – 10) mHz
- Capable of detecting pico-strain level

Highest detection capability

Noise rises below 1 mHz

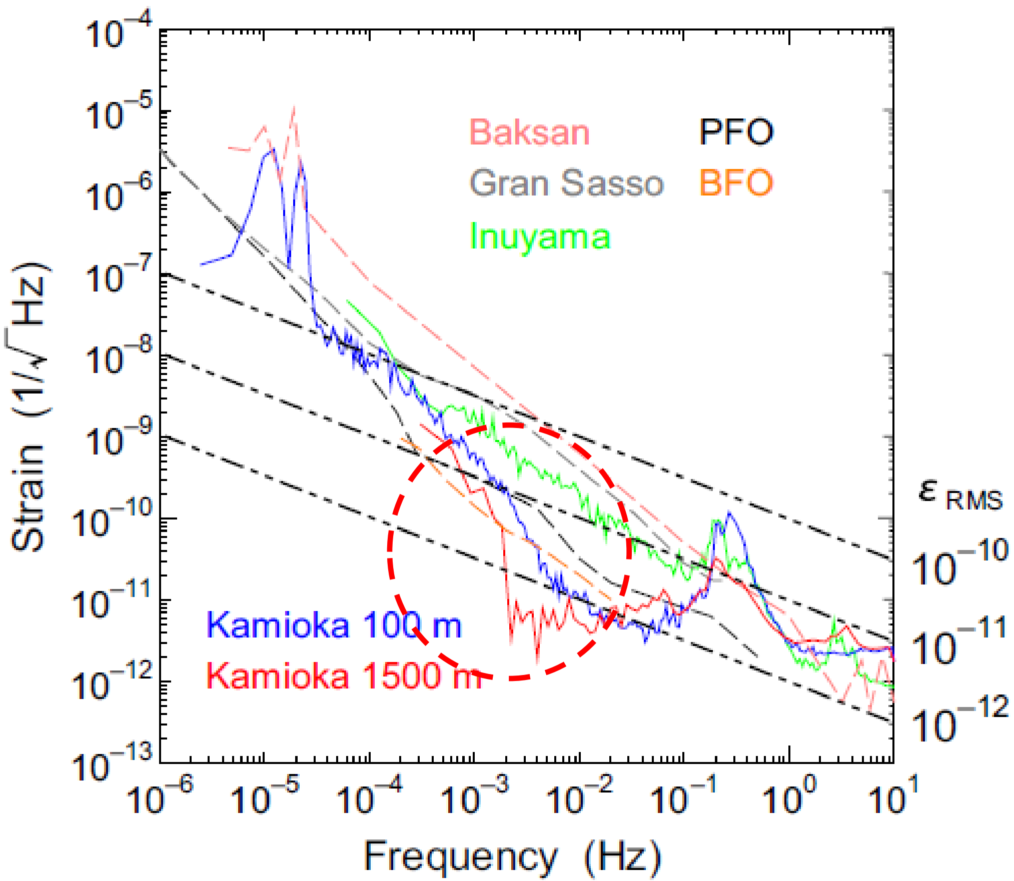

spectra of GIF and other laser strainmeters

Araya et al., EPS, 2017.

Barometric response: a recent study

Strain in $10^{-4} - 10^{-3}$ - Hz region is highly dependent on the air pressure.

Barometric admittance
$\sim 0.55 \times 10^{-9}$ / hPa
cf. $\sim 0.49 \times 10^{-9}$ / hPa (Zürn, 2015)

Air-pressure relative difference between X500 and X2000 stations. Both air pressure are identical (< 10 % difference) below ~3mHz and are uncorrelated above ~10mHz

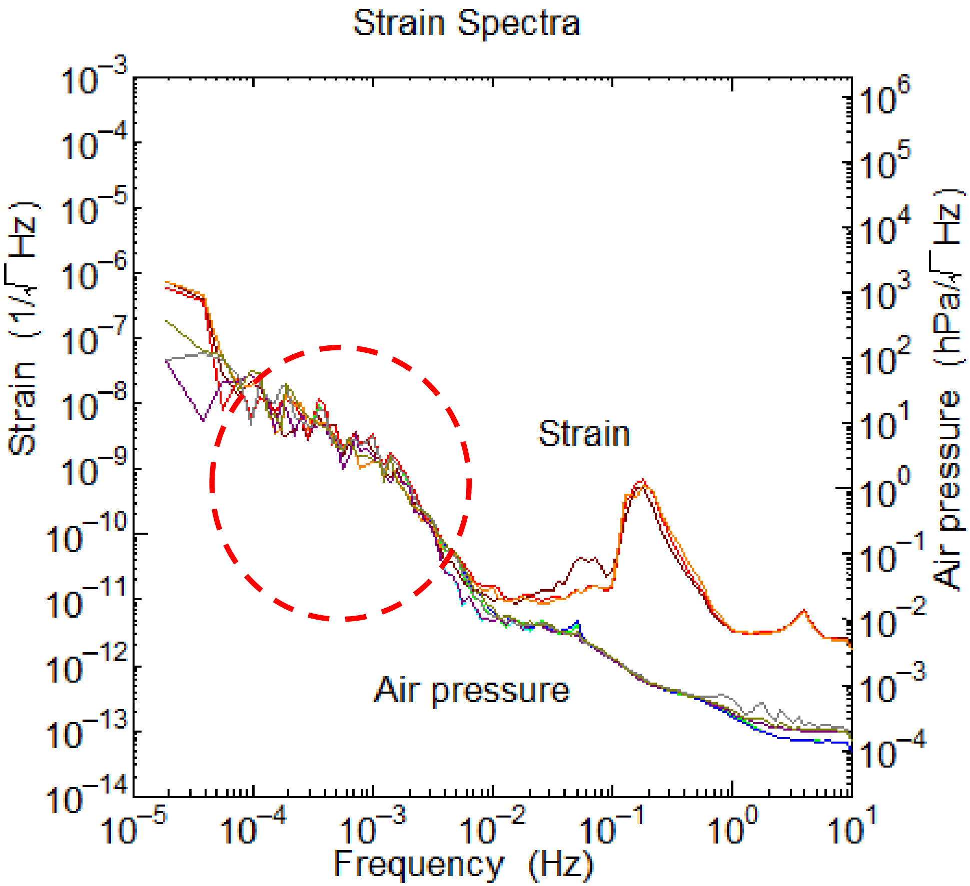

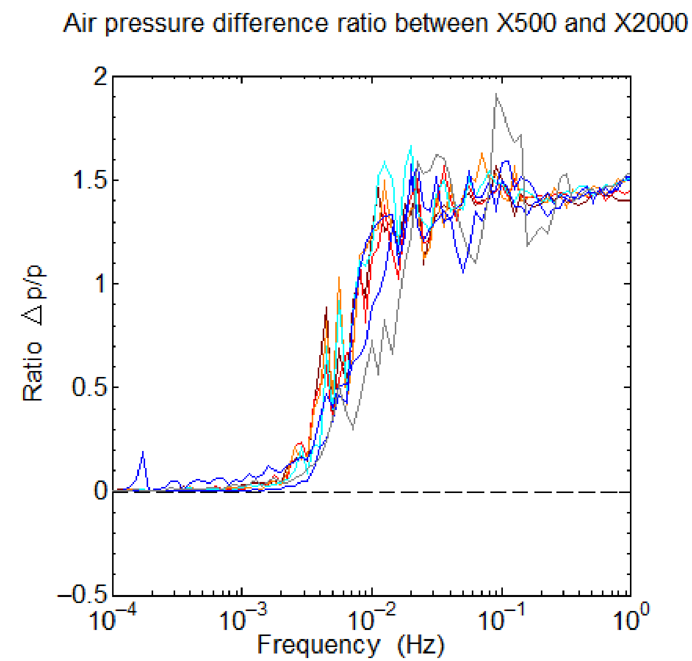

Barometric correction

- Barometric correction reduces strain background to ~1/3 in the $10^{-4} - 10^{-3}$ -Hz region
- The limited reduction implies response of ground to ***regional*** air pressure (not the response of instruments to the ***local*** air pressure).

→ further studies are required

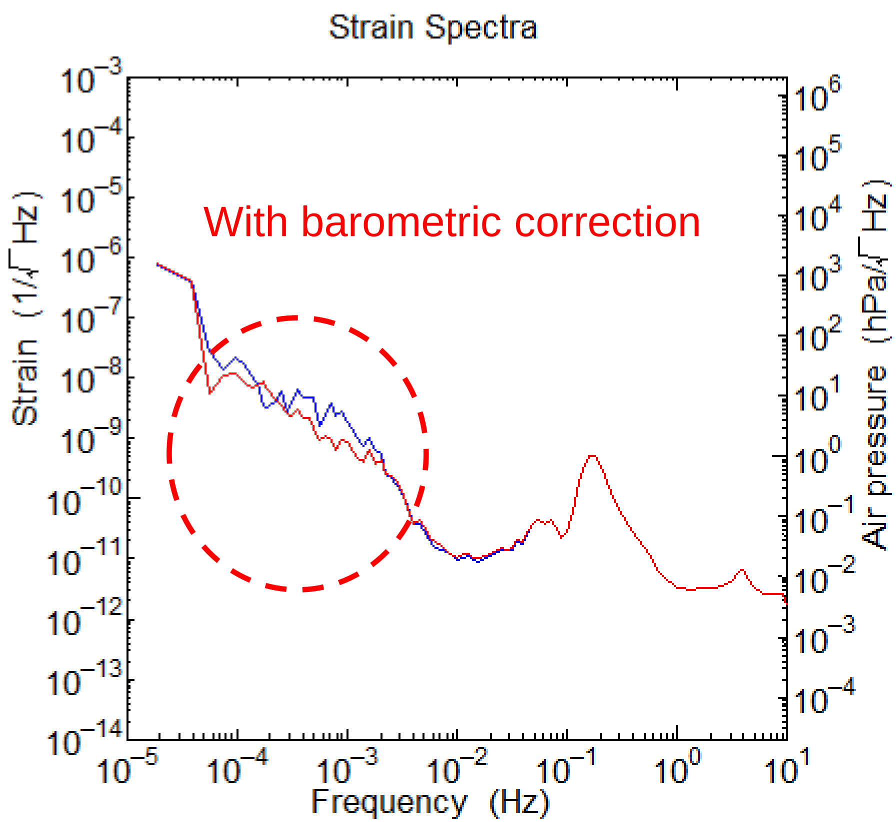

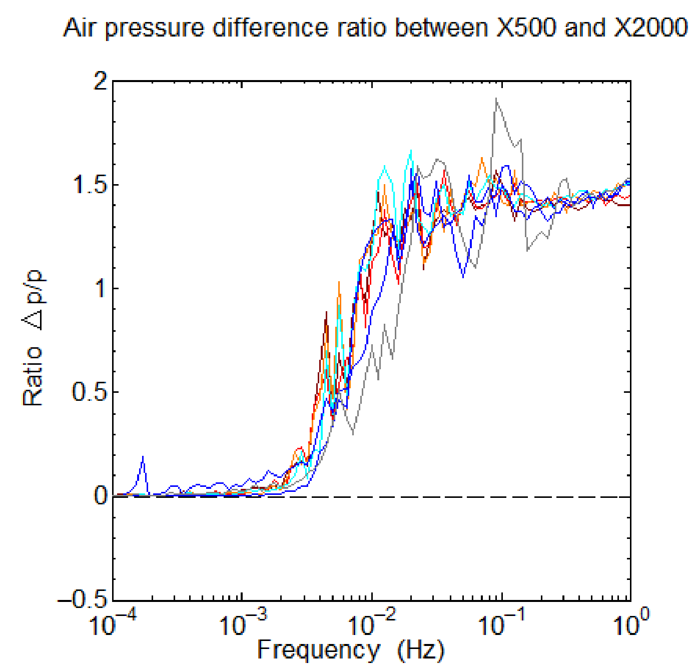

Long-term strains (Jun. – Sep. 2017)

- Baseline shrinks after rainfall (~ 0.1 mm)
  - Averaged for every 10 min.
  - Theoretical tides were calculated and removed.

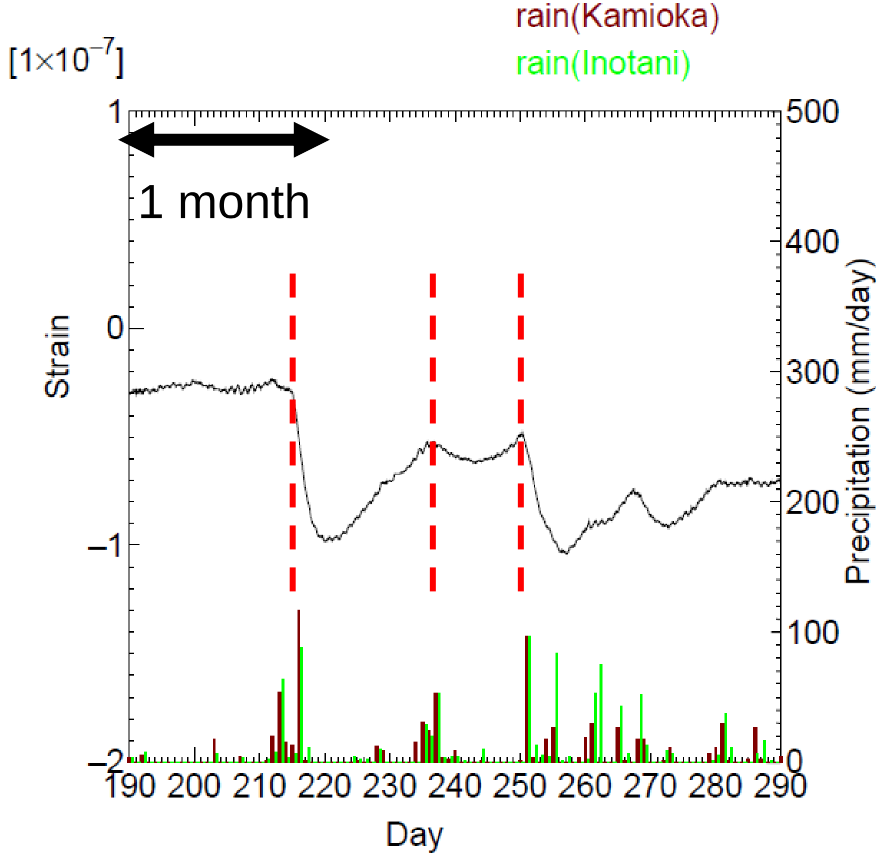

- Response to rainfall
  $\sim 5 \times 10^{-8}$/ 100 mm rainfall
  - due to change in load of groundwater?

→ further investigation

Long-term strains (Dec. 2016 – Feb. 2019)

- Baseline extends after snowfall
  - Study on local crustal motion of KAGRA site
- Response to snow load

$\sim 3 \times 10^{-8} / 1$ m snow depth

→ further investigations required

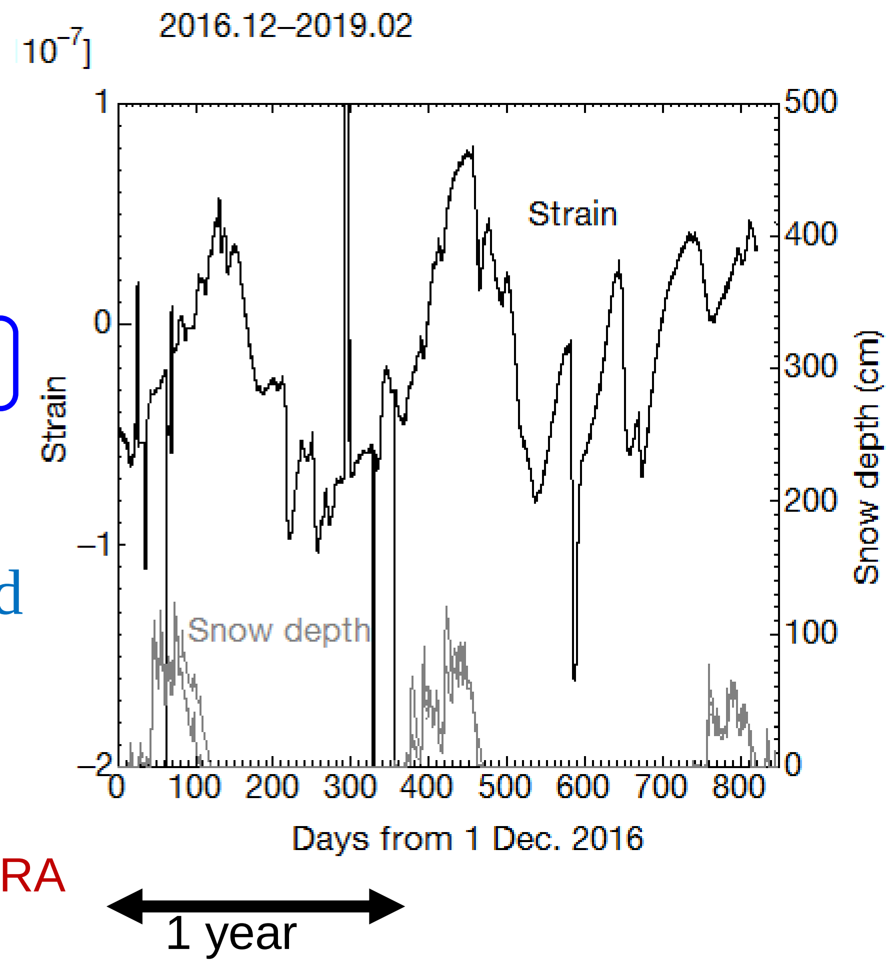

Data of snow depth (not at the KAGRA site) were obtained from AMEDAS (Inotani and Kamioka)

Fault motion monitoring

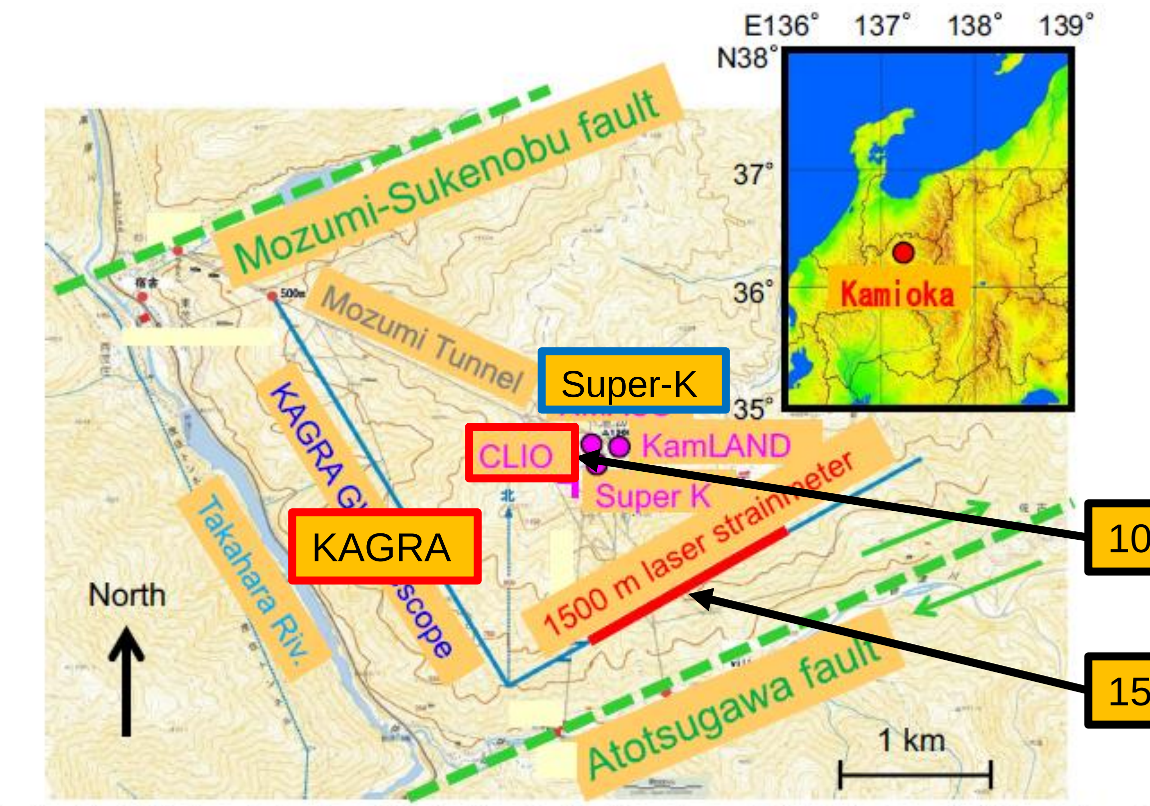

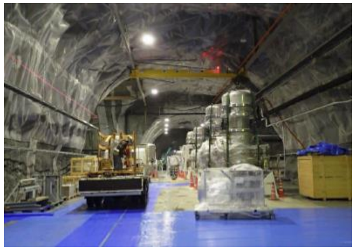

KAGRA baselines and fault locations
(Cosmic Ray Research Institute, Univ. of Tokyo)

Crustal motion observed by GNSS

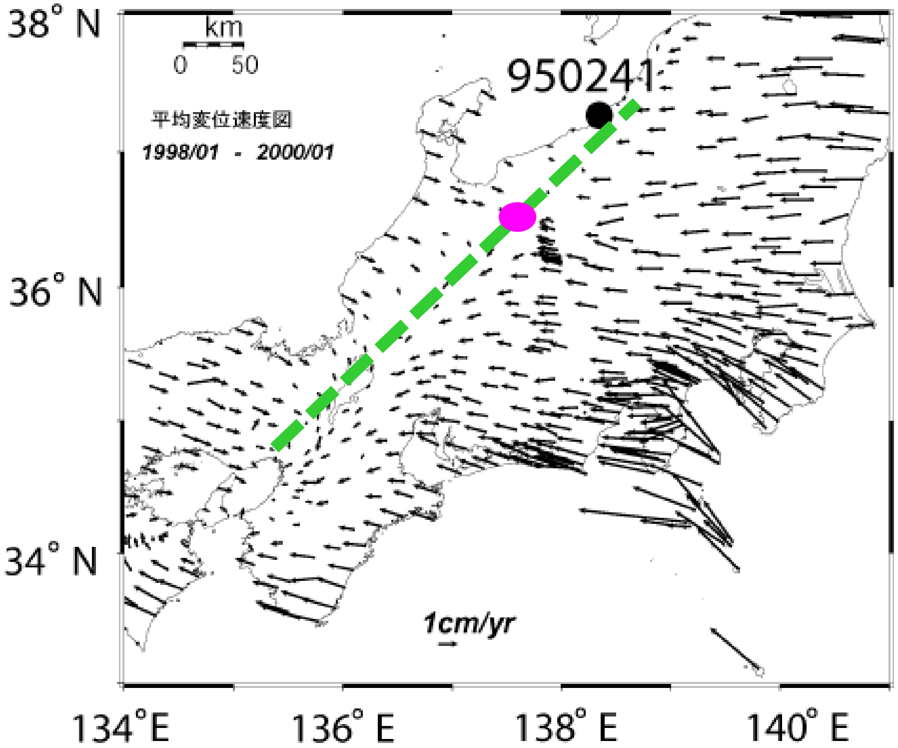

Averaged velocity:
$\sim 10^{-7}$/ year

Niigata-Kobe Tectonic Zone (NKTZ)

Significant to monitor crustal motion precisely over wide timescales.

Long-term strains (Dec.2016 - Feb. 2019)

- Consistent with crustal motion due to plate subduction

Regional ground strain around KAGRA site measured by GNSS

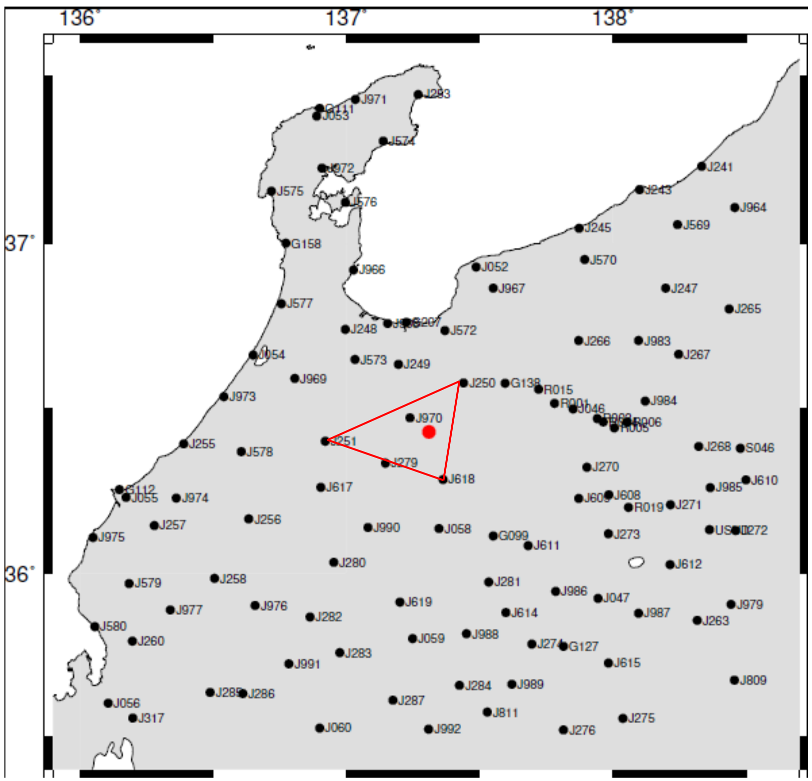

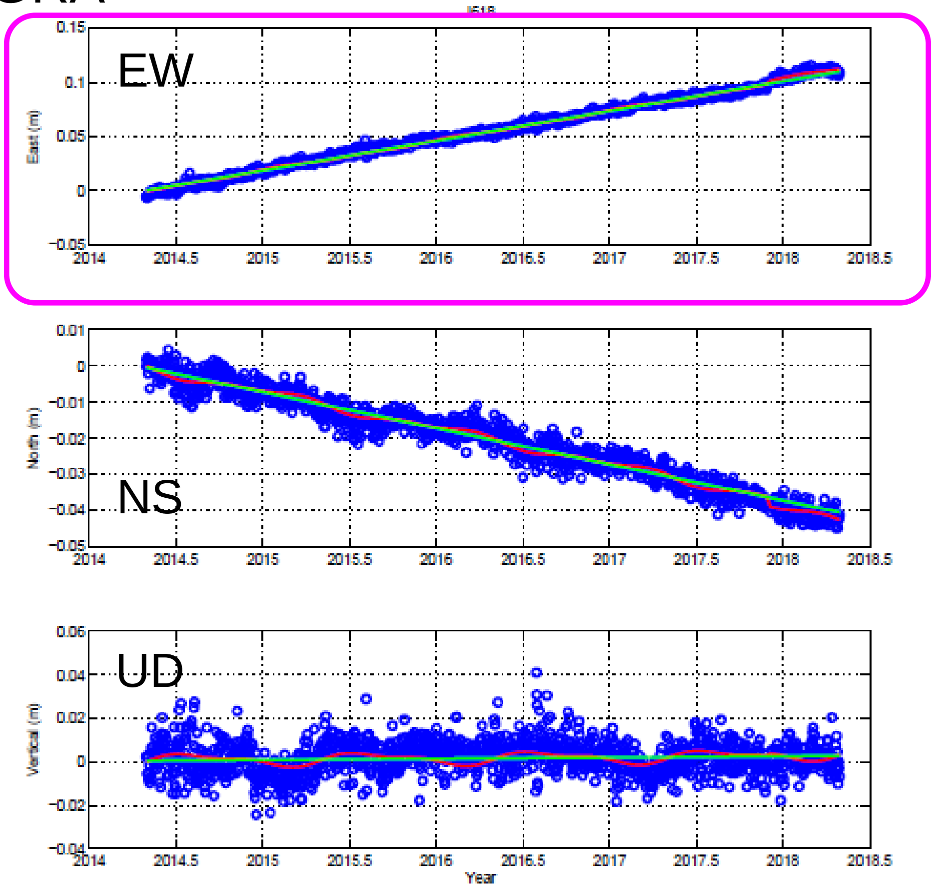

Long-term strains (Dec.2016 - Feb. 2019)

- Consistent with motion due to plate subduction
  - Study on relations between crustal deformation and earthquakes and volcanic activities

GNSS estimates:

Trend: $\sim 7 \times 10^{-8}$ /year

Seasonal change: $\sim 6 \times 10^{-8}$

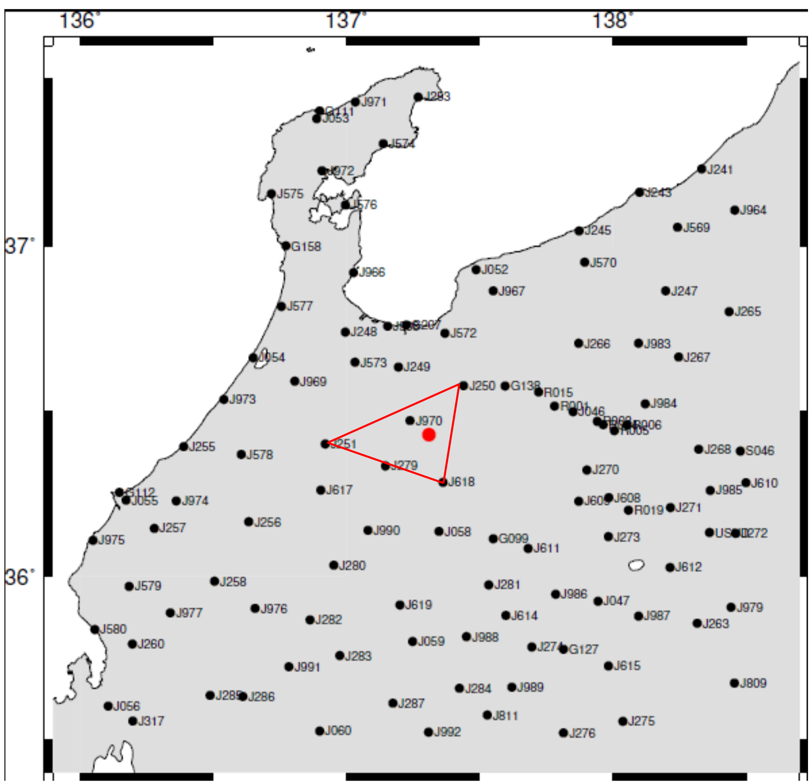

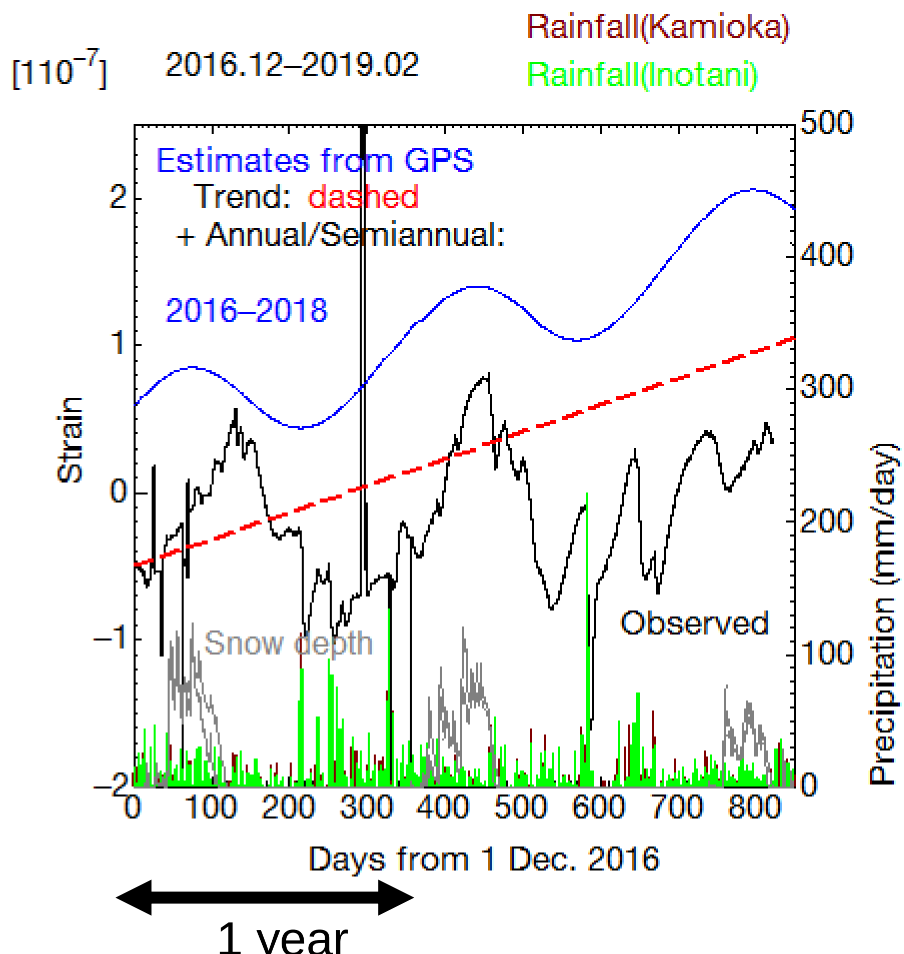

Trend estimated from GNSS (2015.5-2018.4): $\sim 6.7 \times 10^{-8}$ /year (calc. by Fukuda, J)

Study on slow earthquakes and fault motions in Kamioka

- Slow slips around the faults (?)

→ GIF can observe ground motion in very wide time scale

Slow earthquakes and time scale

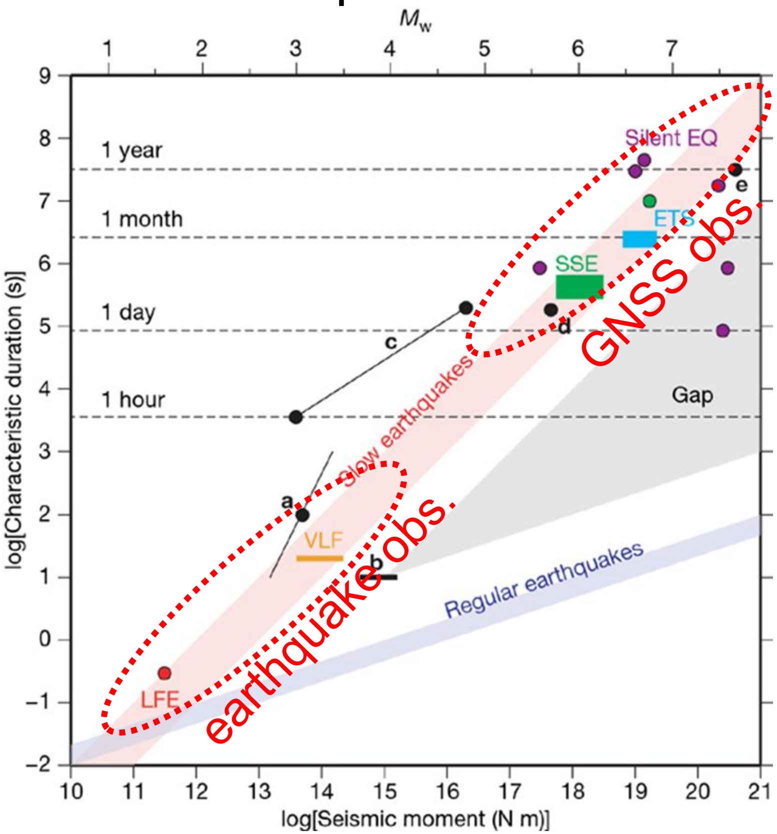

Plate boundary in Nankai trough

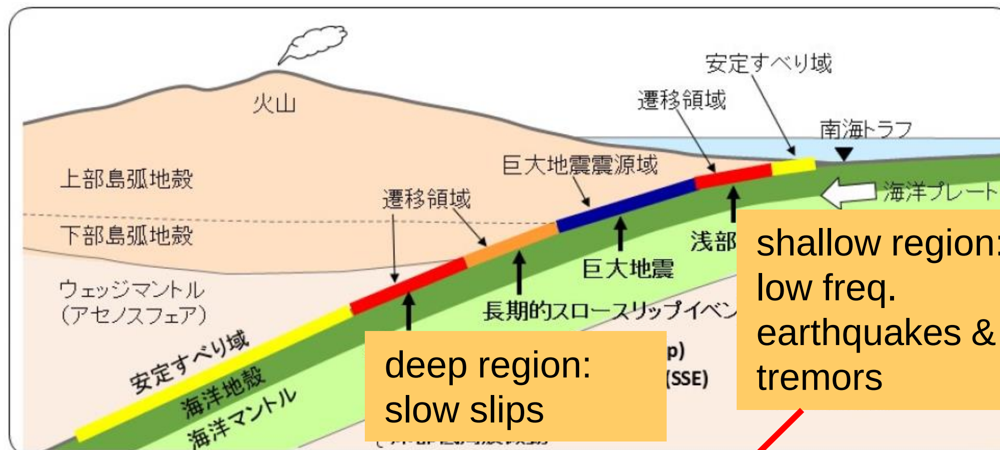

deep region: slow slips

shallow region: low freq. earthquakes & tremors

図１．南海トラフのプレート境界特性と多様なスロー地震分布を模式的に示した断面図

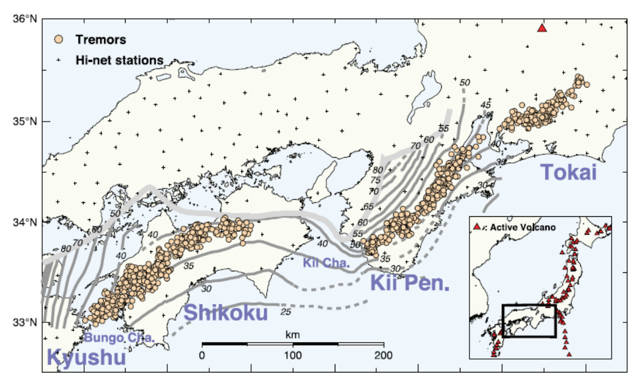

Tremors observed by seismometer-array (Hi-net)

Observation of slow slip events in Tokai-region

Short-term SSE
3-11 Feb. , 2019

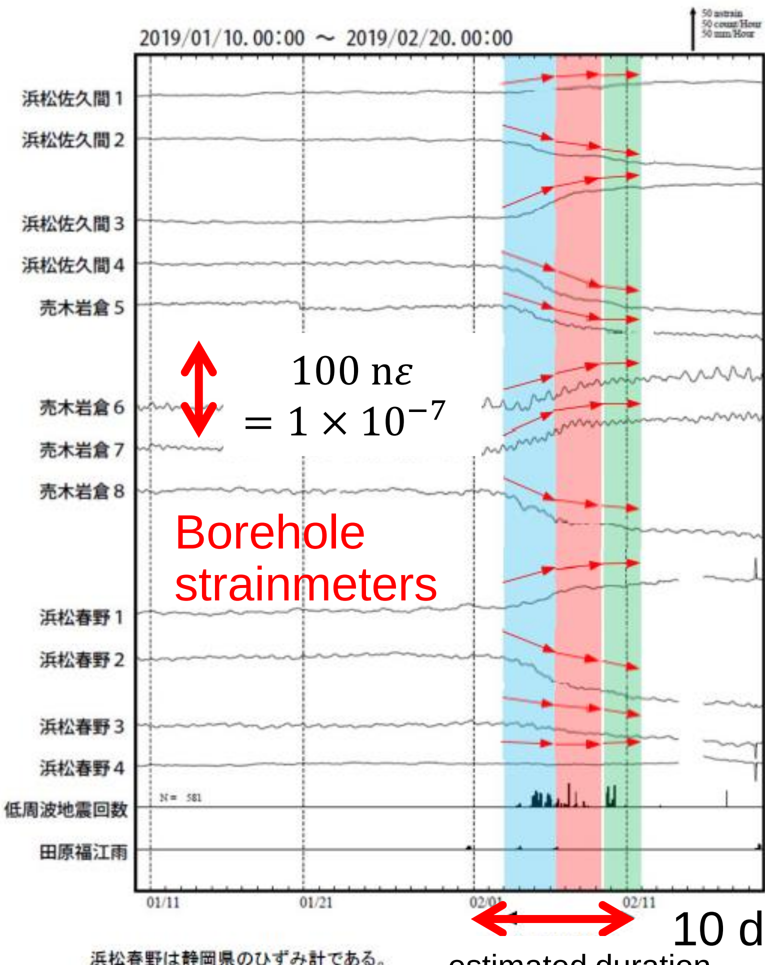

10 days
estimated duration

JMA (2019)

Laser strainmeter at Funagira

- 400 m baseline
- same laser system as GIF

Kamioka

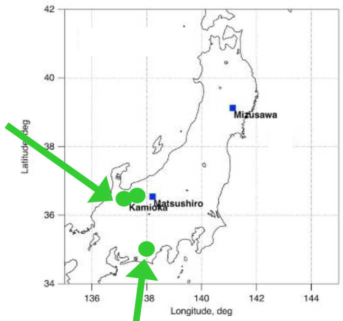

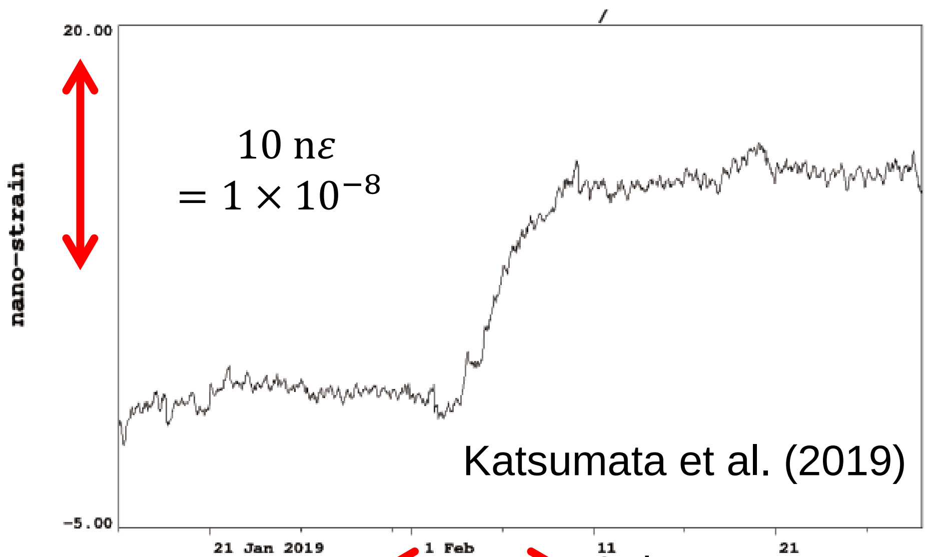

10 days

Katsumata et al. (2019)

Unexplained phenomenon 1

- High frequency oscillation observed with earthquake (25-JUN-2017, NAGANO)…rumbling sound?

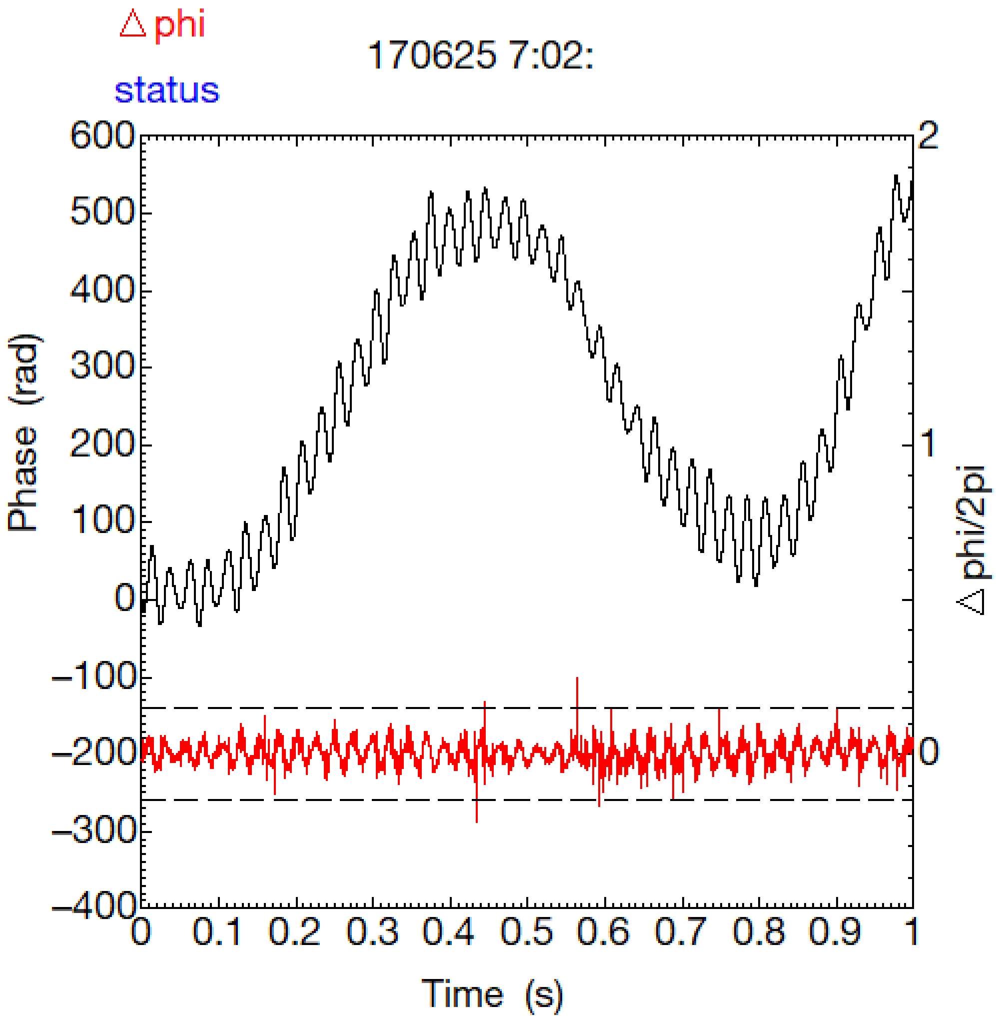

Unexplained phenomenon 2

- Earthquake swarm (?) observed with seismic monitor (PEM) of KAGRA…”wriggles” of ground?

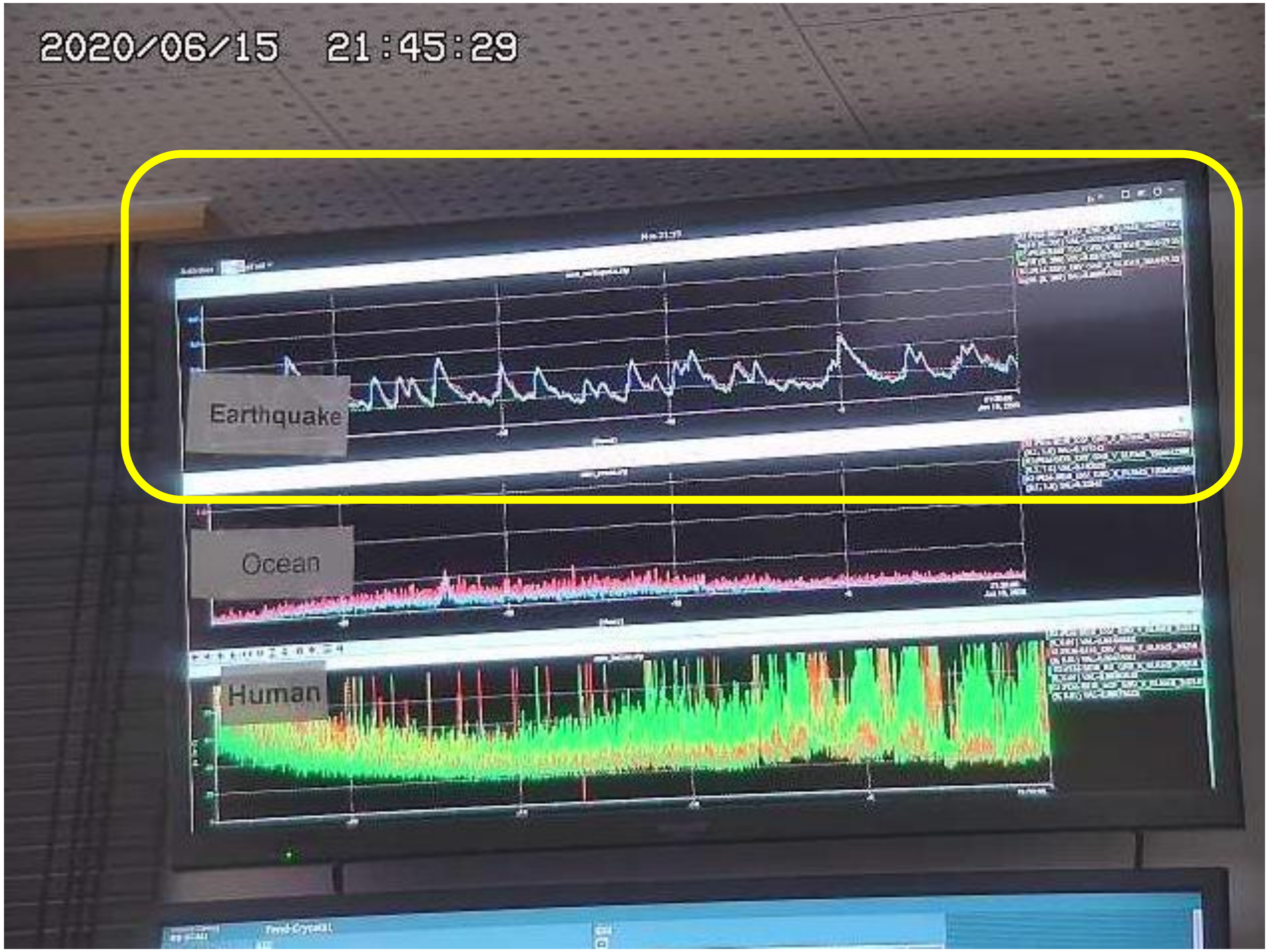

Feedforward control of arm length of KAGRA using GIF signal

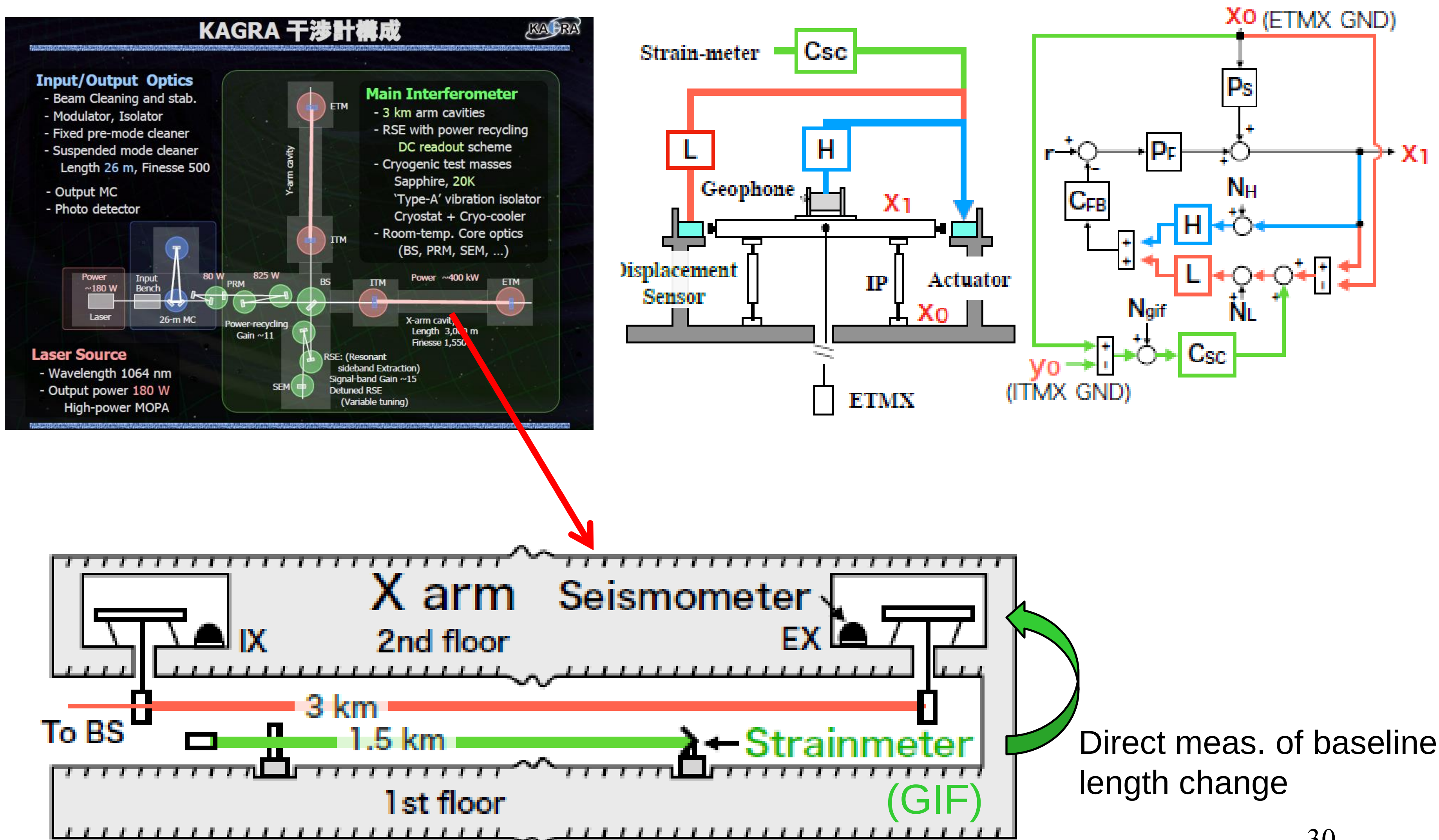

Feedforward control of KAGRA's arm length using GIF signal

T. Akutsu et al., PTEP, 2021

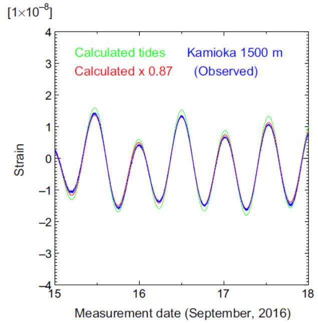

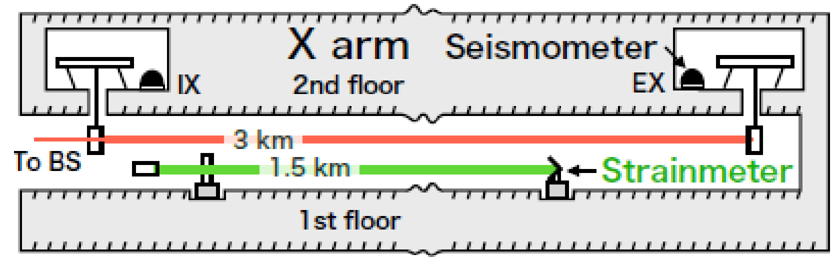

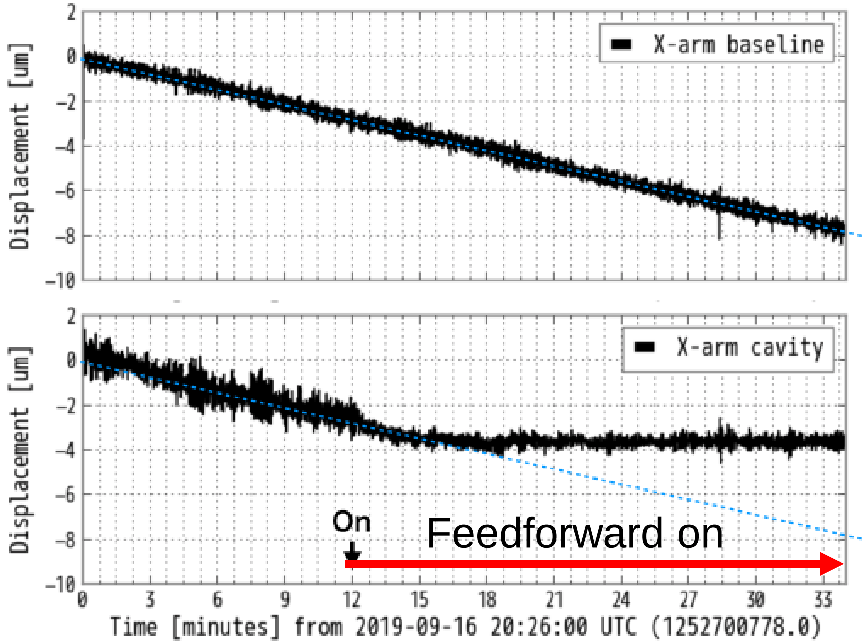

Baseline motions (Earth tide) observed by the GIF (top) and the change in length of the KAGRA X-arm cavity (bottom).

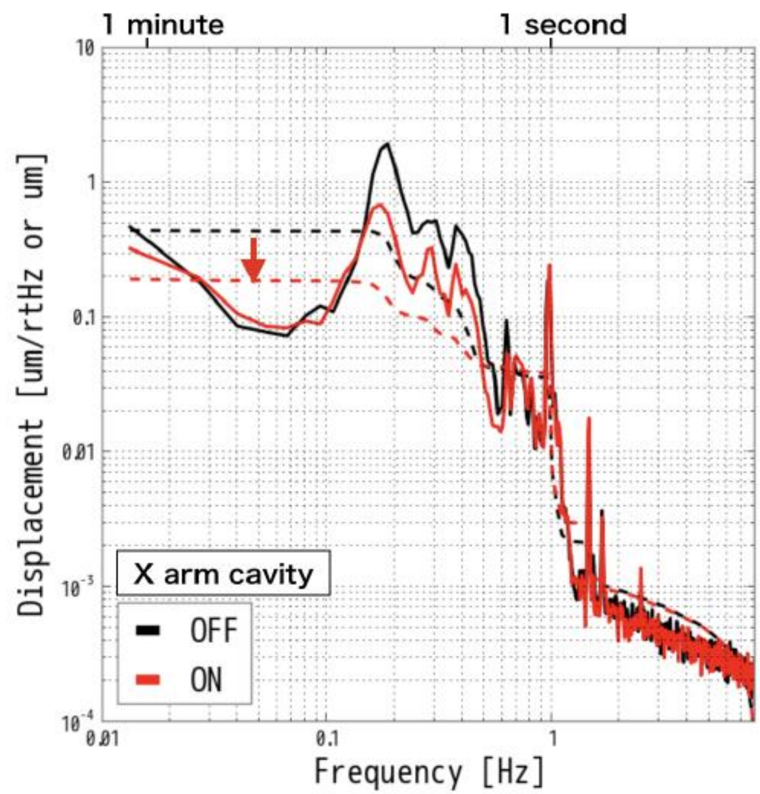

RMS of arm length variation reduced to ~50 %

Improve stability of KAGRA by using GIF data

- Microseism (~0.2 Hz)
  - Ground motion excited by ocean waves
  - Dominant source of RMS motion of KAGRA arm cavity length change

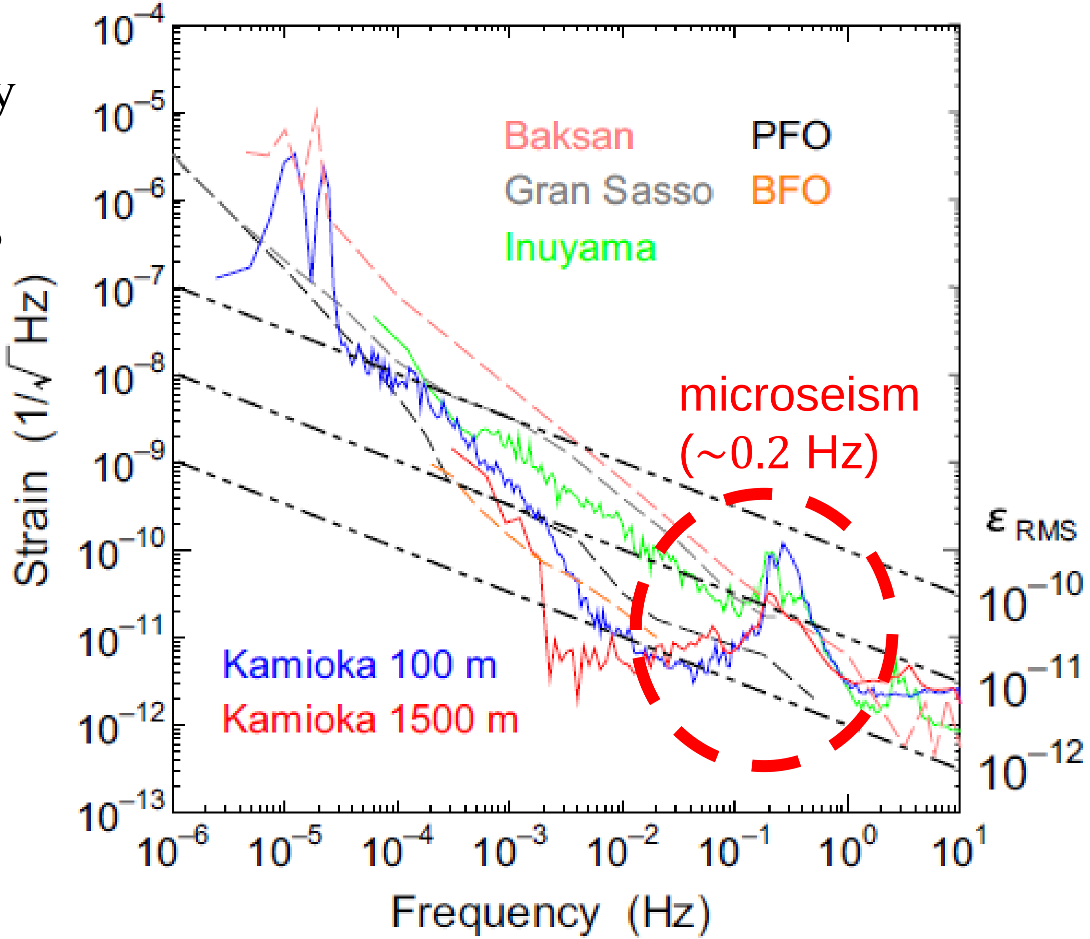

Operation instability of CLIO prototype GW detector associated with increased microseisms due to bad weather condition.

Microseisms (~0.2 Hz) is the enemy.

for stable operation of GW detectors

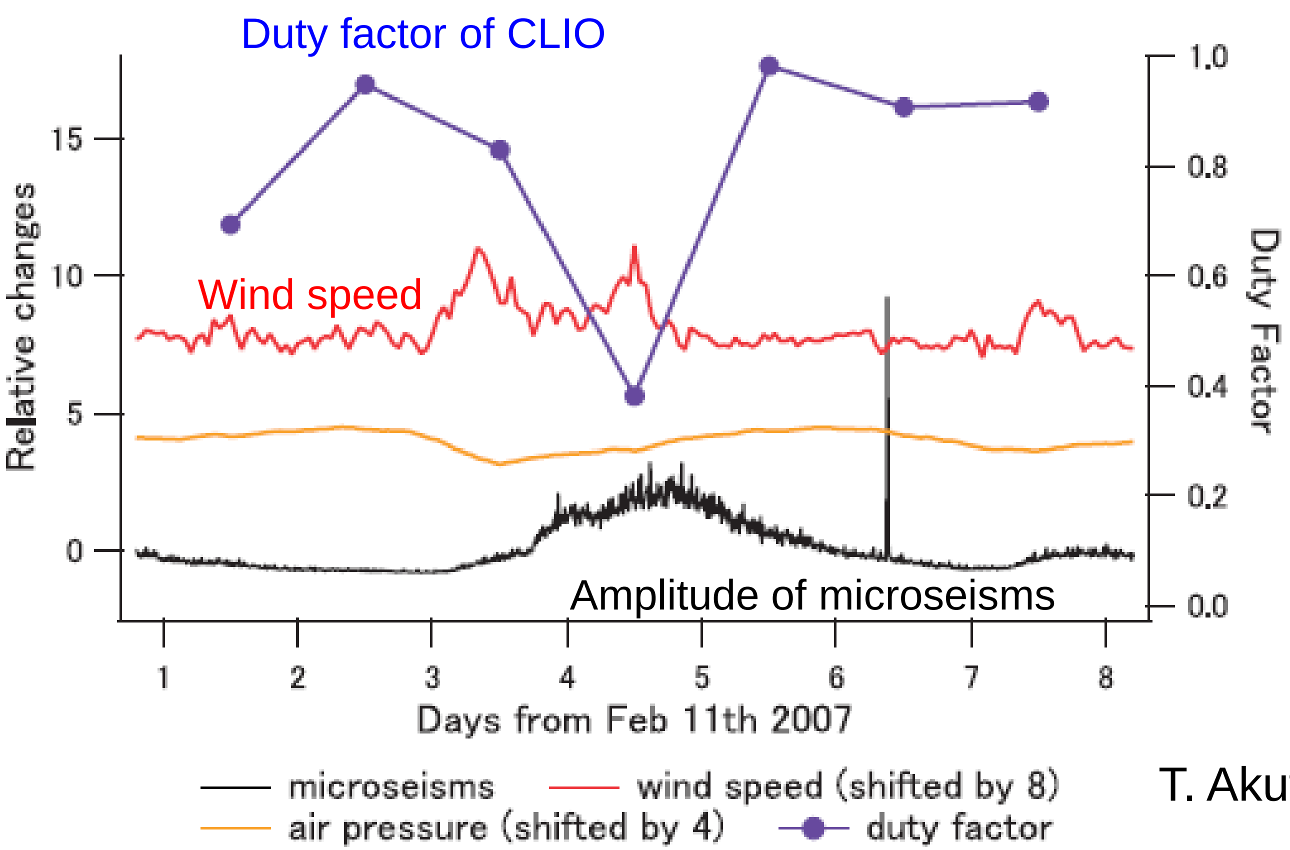

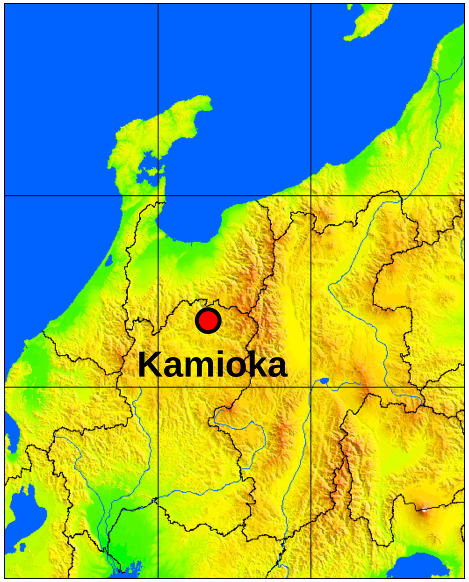

T. Akutsu et al., PTEP, 2018

→ Could be mitigated by feedforward control with GIF data

Research subjects related to GIF subgroup

- Geophysical studies
  - Use of GIF data for studies on inner structure of Earth, crustal motion, and earthquakes etc.
- Studies on environmental effects in KAGRA
  - Barometric changes, rainfalls, microseisms, and earthquakes etc. ...PEM subgroup
- Integration of GIF with KAGRA control system
  - To realize stable GW observation …VIS subgroup